



**POLITECNICO
DI TORINO**

Modeling and Design of Variable Stiffness and Geometry Wind Turbines

Master in Mechatronics

Andrés Fernando Sánchez Castellar

Relatore: Bracco Giovanni

External Relator: Muscolo Giovanni Gerardo

Politecnico Di Torino

Department of Mechanical and Aerospace Engineering

2021

ACKNOWLEDGEMENTS

I mainly dedicate this degree project to God. I want to express my gratitude to God, who with his blessing always filling my life and all my family for always being present.

Finally, I want to express my greatest and sincere gratitude to my parents who have supported me with love and patience. Thank you for instilling in me the example of effort and courage.

I will be missing pages to thank the people who have been involved in carrying out this work. In these lines I want to thank all the people who made this research possible and who in some way were with me in difficult, happy, and sad moments. These words are for you.

To my parents Didier Sanchez Reinoso and Rosirys Castellar Garcia, for giving me the opportunity to train at this prestigious university and having been my support throughout this time, they have patiently always pushed me to achieve my goals without giving up at any time.

In a special way to my thesis tutor, for having guided me in the preparation of this degree work, infinite thanks for having given me the support to develop professionally.

I also want to thank the Università Politecnico di Torino, managers and professors for organizing the Master's program in Mechatronics, especially to my advisers for transmitting their professional knowledge and making this achievement possible, I learned a lot from all of you.

Thanks to my partner Tibisay Ortiz Hernandez who has never stopped pushing me, encouraging me and supporting me even when situations became difficult, thanks for the advice and for being with me even in the distance, helping me in absolutely everything to successfully complete the thesis. You have been vital in this process.

My deep thanks to my brother Daniel Sanchez Castellar, who has been exemplary, thank you for always supporting me, for making me smile and filling me with joy.

I feel very happy because they never stopped believing in me, because even in distance, they were always with me transmitting positive energy, giving me encouragement, helping me to follow the path day after day regardless of adversity, all of you who joined forces to give me encouragement. I don't have enough words to express my appreciation.

Thanks to Maria Isabel who has given me advice and help that given me the opportunity to complete this thesis.

My thanks to everyone, my family, friends who in one way or another, gave me their collaboration and were involved in this project.

ABSTRACT

With the climate change the use of renewable energies is becoming a more important factor every day, that is why the use of this energy is constantly evolving in order to make the most of it. The objective of the following work is the design, modelling and simulation of a vertical axis wind turbine called Savonius, which would present the ability to change the geometry and stiffness of its blades depending on the wind speed. This is to obtain a vertical wind turbine that can take advantage of the energy of the wind in areas where its speed varies, thus generating as much energy as possible. Models and simulations will be carried out with the Ansys Software of various 2D models and then proceed to 3D simulations and select the best blade geometries for low and high wind speeds. With the results, we proceed to present the ways in which a turbine could change its geometry, together with their respective designs generated with the Solid Edge software.

Keywords: Variable geometry, variable stiffness, Savonius turbine, wind energy, turbine simulation

CONTENT

ACKNOWLEDGEMENTS.....	i
ABSTRACT.....	ii
FIGURE LIST.....	v
TABLE LIST.....	vii
LIST OF ACRONYMS AND SYMBOLS.....	viii
INTRODUCTION.....	1
1. STATE OF ART.....	3
1.1. RENEWABLE ENERGIES.....	3
1.2. WIND ENERGY.....	4
1.3. WIND TURBINES.....	4
1.4. VERTICAL AXIS WIND TURBINES.....	6
1.5. SAVONIUS TURBINE.....	6
1.5.1. GEOMETRIC PARAMETERS OF THE ROTOR.....	7
1.5.2. PERFORMANCE PARAMETERS OF A SAVONIUS TURBINE.....	9
1.5.3. PERFORMANCE IMPROVEMENT OF THE SAVONIUS TURBINE.....	12
1.5.4. SAVONIUS ROTORS OF VARIABLE GEOMETRY.....	13
1.5.5. SIMULATION OF SAVONIUS TURBINES.....	15
1.5.6. STATISTICAL METHODS.....	17
1.6. EQUIPMENT FOR AUTOMATION.....	19
1.6.1. ACTUATORS.....	19
1.6.2. MICROCONTROLLERS.....	19
1.6.3. SENSORS.....	20
2. METHODOLOGY.....	20
2.1. ROTOR DESIGN.....	20
2.1.1. PROFILE SELECTION.....	22
2.1.2. SIMULATION 2D.....	22
2.1.3. SIMULATION 3D.....	25
2.1.4. GEOMETRIC DETAILS OF THE ROTOR.....	26
2.1.5. OPTIONS TO CHANGE THE TURBINE GEOMETRY.....	28
3. RESULTS.....	29
3.1. SIMULATION 2D RESULTS.....	29
3.2. COMPARISON OF ROTORS BY POWER GENERATION.....	34
4. RESULTS FOR CHANGING THE TURBINE GEOMETRY AND STIFFNESS.....	36
4.1. PROPOSED SOLUTIONS.....	36
4.1.1. SOLUTION 1.....	36
4.1.2. SOLUTION 2.....	38
4.1.3. SOLUTION 3.....	39
4.1.4. SOLUTION 4.....	39

4.2. NUMERICAL ANALYSIS OF THE PROPOSED SOLUTIONS.....	41
4.3. DESICION MATRIX.....	42
4.4. SYSTEM OPERATION FOR THE CHANGE OF GEOMETRY.....	44
4.4.1. SYSTEM OPERATION FOR SOLUTION 1 AND 3.....	44
4.4.2. SYSTEM OPERATION FOR SOLUTION 2.....	45
4.4.3. SYSTEM OPERATION FOR SOLUTION 4.....	45
4.5. SOLUTION COST.....	46
4.5.1. BLADES.....	46
4.5.2. ACTUATORS.....	46
4.5.3. SENSORS.....	47
4.5.4. MICROCONTROLLERS.....	48
4.5.5. OTHER MATERIALS.....	49
4.6. COST SUMMARY.....	50
4.7. FUTURE WORK AND DISCUSSIONS.....	51
5. CONCLUSIONS.....	54
6. BIBLIOGRAPHY.....	56

FIGURE LIST

1.1 Figure 1 Vertical axis wind turbine of 150 kW, INER-P150II. [28].....	5
1.2 Figure 2 Vertical axis wind turbines [33].....	6
1.3 Figure 3 Conventional Savonius Turbine [34].....	7
1.4 Figure 4 Geometric Parameters of a Savonius rotor [16].....	8
1.5 Figure 5 Power coefficient curves for wind turbines [33].....	13
1.6 Figure 6 Rotor working principle proposed by Sobczak [50].....	15
1.7 Figure 7 3D mesh with 5 million elements [61].....	17
2.1 Figure 8 Effect of aspect ratio on the performance of a Savonius rotor [74].....	21
2.2 Figure 9 Geometry for profile simulations. Own elaboration.....	23
2.3 Figure 10 General (left) and detailed (right) views of the mesh for profile simulations. Own elaboration.....	23
2.4 Figure 11 Geometries 1 (blue) and 2 (orange). Own elaboration.....	24
2.5 Figure 12 Comparison of the experimental power curves and those obtained by means of CFD [76].....	26
2.6 Figure 13 - Other geometric details of the rotor.....	27
2.7 Figure 14- Geometric details of the rotor for solution 3.....	28
3.1 Figure 15 Power coefficient for various X coordinate values of the control point. Own elaboration.....	29
3.2 Figure 16 Power coefficient for various values of Y coordinate of the control point.....	30
3.3 Figure 17 Behavior of the flow in the profile at different points of the rotation (Geometry 2, for a speed of 10 m/s at a TSR of 0.8). Own elaboration.....	30
3.4 Figure 18 Profile pressure contour at different points of rotation (for a speed of 10 m/s at a TSR of 0.8).....	31
3.5 Figure 19 Power curves for the different geometries and the designed rotor.....	32
3.6 Figure 20 Current lines on the rotor. Own elaboration.....	33
3.7 Figure 21 Pressure contour in the rotor when the wind hits the blades head-on. Viewed from the front (left) and viewed from behind (right). Own elaboration.....	34
3.8 Figure 22 Probability distribution for wind speed in Medellín [77].....	35
4.1 Figure 23 Isometric view of solution 1. Own elaboration.....	37
4.2 Figure 24 Bottom view of the solution 1. Own elaboration.....	37

4.3 Figure 25 Separated turbine by its two pieces, B (bottom piece) is the base and A (top piece) is the piece to be changed (there will be two A pieces but with different geometries). Own elaboration.....	38
4.4 Figure 26 View of the blades with their two shapes that it acquires depending on the wind speed. Own elaboration.....	39
4.5 Figure 27. View of blades (made with fabric) next to the springs (blue).....	40
4.6 Figure 28 - Comparison of the performance of the different proposed solutions.....	41
4.7 Figure 29 Pneumatic cylinder actuator. Image taken from the Festo catalog.....	47
4.8 Figure 30 PCE-FST-200-201 Wind Sensor. Image taken from the pce-instruments catalog.....	47
4.9 Figure 31 Normally Open Inductive Proximity Sensor. Image taken from the Amazon catalog	48
4.10 Figure 32 Arduino microcontroller. Image taken from the Amazon catalog.....	49
4.11 Figure 33 Flexible waterproof polyester fabric. Image taken from the Amazon catalog.....	49

TABLE LIST

2.1 Table 1 – Geometric parameters of the rotor. Own elaboration.....	22
2.2 Table 2 – Mesh independence study.....	23
2.3 Table 3 – Characteristics of the first 9 evaluated profiles.....	24
2.4 Table 4 – Characteristics of the profiles evaluated with smaller variations in geometry.....	25
3.1 Table 5 – Design rotor performance.....	31
3.2 Table 6 – Annual production of geometry 1 and 2 and the variable rotor.....	35
4.1 Table 7 –Decision matrix for each proposed solution.....	43
4.2 Table 8 - Table Values of each element together with the total for each solution.....	50

LIST OF ACRONYMS AND SYMBOLS

Symbol	Term	Unit SI
C_p	Power coefficient	
C_{max}	Max curvature of the profile	
L	Lift force	[N]
U_∞	Fluid velocity	[m s ⁻¹]
D	Drag force	[N]
V	Velocity	[m s ⁻¹]
A	Reference body area	[m ²]
C_L	Lift coefficient	
C_D	Drag coefficient	
y^+	Dimensionless wall distance	
R	Rotor radius	[m]
R_e	Reynolds	
c	Chord	[m]
w	Relative velocity	[m s ⁻¹]
N_b	Number of blades	
n	Number of sections	
r_n	Local radius	[m]
n_a	Actual section	
c_n	Optimal chord section	[m]
a	Axial induction factor	
a'	Tangential induction factor	
dF	Component of the force that the flow produces in each section	[N]
P	Power	[W]
t	Height of the cube	[m]

INTRODUCTION

The world faces a huge challenge due to energy shortages, environmental pollution and the emission of greenhouse gases [1]. In the IPCC Special Report, it is shown that there was a global warming of 1.5 ° C, the authors indicate that the temperature change was higher than expected; furthermore, they conclude that immediate changes are required [2]. Authors such as Nieburhr agree that a transition to a renewable energy grid that significantly reduces carbon emissions should be made in the next decade [3]. Renewable energies are a type of technology through which cleaner energy can be obtained than the one obtained through traditional sources of fossil energy; for this reason, they are a reliable source to reduce the emission of greenhouse gases. In particular, they can provide a cost-effective source of energy in local rural areas where distances to the central power grid are often large, also in small towns where energy demand is relatively low [4]. There are several types of renewable energy: solar, wind, hydro, etc. Wind energy is an inexhaustible renewable energy source that is produced from the wind, for this reason, the generation of energy from this resource reduces the use of fossil fuels. Unlike solar power that is only available during the day and dependent on environmental conditions, or hydropower that is available in specific locations, wind power is available virtually anywhere, anytime, helping to reduce the amount of energy and the creation of local jobs [5].

Savonius turbines are simple horizontal axis wind turbines useful for extracting energy from the wind. But due to the low efficiency of Savonius rotors, attention has been paid to the design of these turbines to improve their performance. Several studies have been carried out in order to find a geometry that allows maximizing the efficiency of this type of rotors. Several studies have been developed to improve turbine performance with different variations of its geometry [6]. Simple changes such as the use of plates at the ends of the blades [7], [8], allow an increase in efficiency. Similarly, there are optimal values for the turbine overlap ratio (the fraction of the diameter shared by the blades), between 0.1 and 0.7 depending on the speed regime at which the turbine operates [9] - [13]. One of the geometric variations that has been most successful in improving the efficiency of this type of rotor is the implementation of deflectors, curtains or barriers [14] - [17]. Plates are placed around the rotor to control the flow, so that it is more directly on the advancing blade, and if possible, accelerate it [18]. Some success has been achieved with this proposal [19] - [21], reaching efficiency values of up to 0.51. Although these types of improvements make turbines more efficient, these mechanisms make the performance of the rotor dependent on the direction of the wind, so systems are required to rotate the turbine facing the wind, thus increasing the complexity of the design and the cost of its operation and maintenance.

Taking into account the above, then it is evident the need to propose and evaluate alternatives that allow mitigating the main disadvantage of Savonius turbines, which is efficiency, and at the same time prevent them from losing their main advantages such as facility of manufacture, operation, maintenance, independence of performance to the direction of the wind, and its few structural limitations. An alternative to obtain a greater advantage from Savonius turbines is to have them change their geometry depending on the speed of the wind, so that the most of it is taken throughout its operational range. In this way, the design of a Savonius rotor that is not optimized

for a single operating condition is proposed, but with a versatile design, allowing its geometry to change conveniently for different wind speeds. In this way, greater advantage can be taken in urban applications where the wind is highly variable and unpredictable, while maintaining a simple design whose performance remains independent of the wind direction.

1. STATE OF ART

1.1 RENEWABLE ENERGIES

Global warming is caused by environmental pollution that has generated a negative impact on the planet and the living beings that inhabit it, it has been possible to notice climatic changes and the natural phenomena [22]. The increase in temperature both in the atmosphere and in the oceans has been increasing considerably. Obviously in recent years these have been the hottest [23].

Deforestation, the burning of fossil fuels that causes air pollution help to make the damage worse and worse and cause the highest concentrations of greenhouse gases. It must be considered that this problem is even higher in developed countries due to the factories they have. Global warming is produced by multiple causes within these, the emission of carbon dioxide stands out, being a problem of maximum frequency that today is a complete threat to the health of the environment, and this has produced a change the weather around the world [24].

All this means that a very high price is being paid for the actions of man on earth and these are the ones that generate an impact on the deterioration of the environment, thus producing global warming, so with the passing of time, some strategies are being in search and solutions to minimize these damages, playing a decisive role to improve the situation.

Subsequent to the above, product of the need for greater energy efficiency and care for the environment, the increase in the use of renewable energies is born, this being essential for a solution.

Of all the different sources of energy that exist, renewable ones are those that are produced constantly and are inexhaustible, the sun is the origin of all renewable energies, due to the heat that emanates on the earth generates the pressure differences. Which results in the wind that are the source of wind energy. The sun generates the evaporation of water which results in the creation of clouds and therefore rain is generated. Direct energy from the sun is also used, which we know as solar energy and photovoltaics.

As we have seen before, the act of burning fossil fuels to obtain electricity is causing us considerable damage to the environment which causes environmental impacts and produces greenhouse gases (such as carbon dioxide). This causes changes in weather patterns that lead to an increase from droughts, tornadoes and also floods.

Renewable energies are classified as clean energies because the environmental impacts are considerably lower and reversible. It is also said that they are inexhaustible, they produce electricity through solar radiation and do not produce a decrease in the amount of energy that the sun sends to the earth. That also happens with the wind, even with the wind turbines that extract their power to convert it into electricity, it does not cause disorder or disturbances in the thermal balance of the planet.

There is an increasing demand for electricity, it increases and this is depleting fossil fuels, becoming a serious problem. This means that it is very necessary to invest in renewable energies in order to reduce such dependence on fuels and, on the contrary, open the field to inexhaustible and clean energy [25].

1.2 WIND ENERGY

Wind energy is obtained through the wind, it takes advantage of the air masses. This is used specially to produce electricity today, through wind turbines that are connected to the distribution networks of electrical energy. This can generate electricity in regions that are isolated, thus having a great advantage is considered cheaper and more competitive.

Wind energy could provide five times more electricity than the total consumed worldwide, without affecting the areas with the highest environmental value. The power that can be obtained with a wind generator is proportional to the cube of the wind speed; When the wind speed is doubled, the power is multiplied by eight, and hence the average wind speed is a determining factor when analyzing the possible viability of a wind system. Wind energy is a highly variable resource, both in time and place, and can change a lot in very short distances. In general, coastal areas and mountain peaks are the most favorable and best equipped for harnessing the wind for energy purposes [5].

Wind energy has a number of benefits for the environment because it minimizes the impact on climate change. Wind energy is clean since it has low greenhouse gas emissions, also it has a low impact. It is inexhaustible since it is an unlimited resource and constant, where the wind is stronger the benefit are greater [26]

1.3 WIND TURBINES

The wind turbine is considered a mechanical device that converts energy from the wind into electricity. The turbines are designed with blades, these rotate thanks to the force of the wind. For the extraction of energy from the wind, the turbines that are used have two main subcategories: horizontal axis (HAWT) and vertical axis (VAWT), according to the alignment between their axis of rotation and the direction of the wind. Each one has its advantages depending on the application. Horizontal axis turbines are generally more efficient and are more common for medium and large-scale applications [27].

Horizontal axis wind turbines are composed of different elements that allow their operation, some of the main elements are:

- Containment tower
- Orientation system
- Nacelle
- Generator
- Anemometer
- Vane

- Low speed shaft
- High speed shaft
- Blades
- Bushings
- Rotor
- Multiplier
- Electronic controller
- Gearbox

Figure 1 shows the inside of a nacelle of a 150kW wind turbine, in this image you can see some of the elements that are presented in the previous paragraph. You can also see the fully assembled turbine located at the top of the tower. The use of towing equipment to move the nacelle is appreciated, this indicates that this element has a considerable weight.

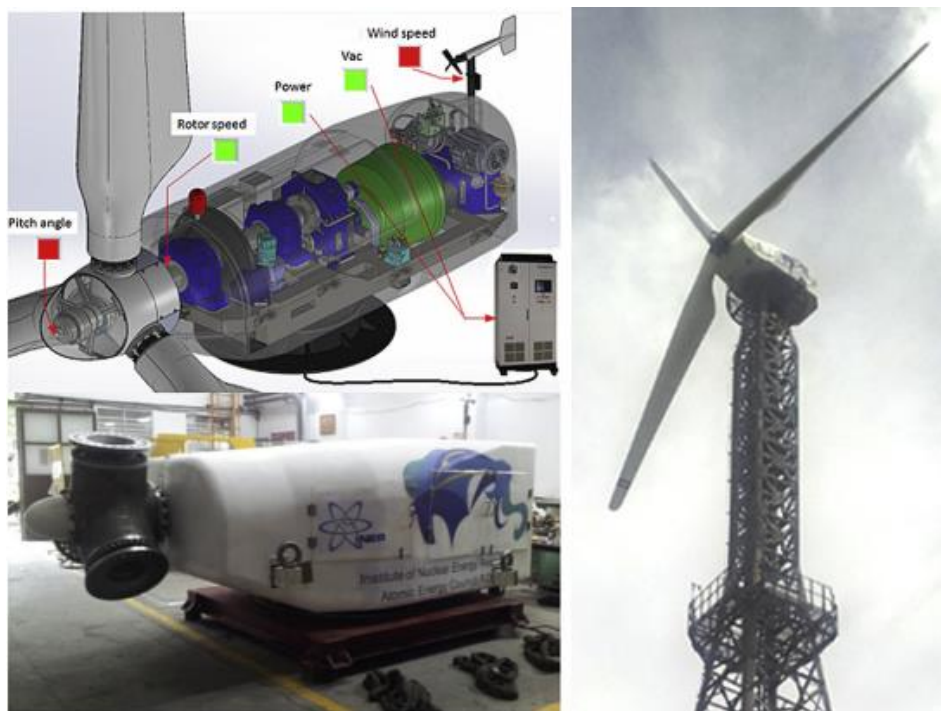


Figure 1 Vertical axis wind turbine of 150 kW, INER-P150II. [28]

Vertical axis wind turbines are used for urban applications where the wind is more variable and less intense, which, despite their lower efficiency, perform much better at low wind speeds and their performance does not depend on the wind direction [29], [30]. These turbines are considered lighter than the horizontal ones and although the wind is weak, they continue to operate at the rate of the wind speed.

1.4 VERTICAL AXIS WIND TURBINES

Vertical axis wind turbines, unlike horizontal axis turbines, do not require a system that keeps the turbine aligned with the direction of the wind, making the design, maintenance and operation more economical. In Figure 2 you can see some of the most common vertical axis wind turbines. The Savonius is a drag turbine that is made up of two discs that support 2 or 3 blades. If viewed from above, an S shape is observed [A3]. The Darrieus is generally composed of two arc-shaped blades that have a certain thickness or a thickness given by an aerodynamic profile. The H Darrieus are a variation of the Darrieus, these are composed of vertical blades that in their cross section are shaped like an aerodynamic profile [31], [32].

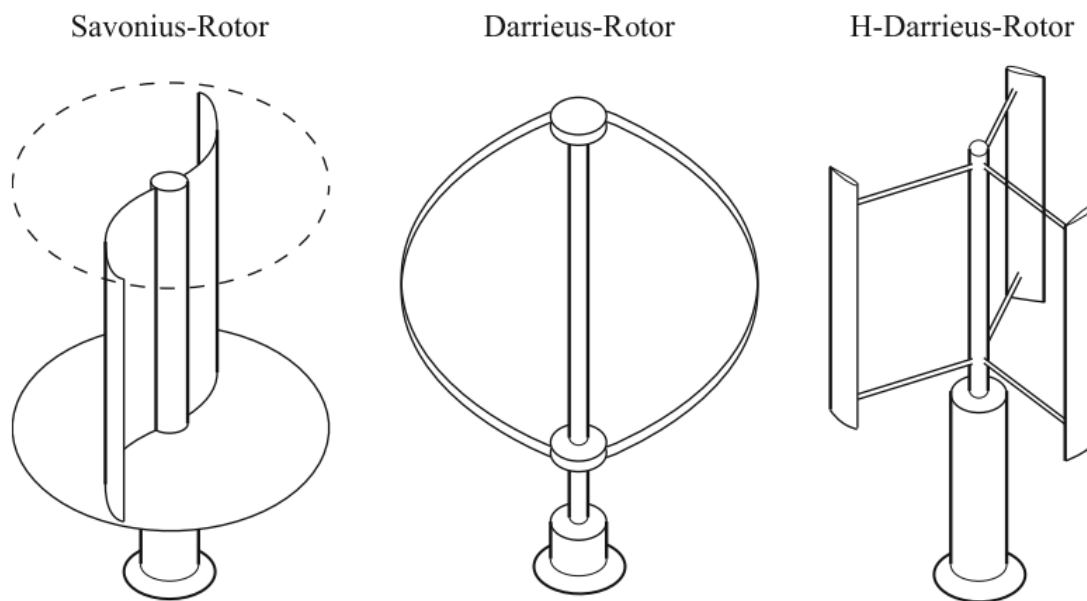


Figure 2 Vertical axis wind turbines [33]

1.5 SAVONIUS TURBINE

As mentioned above, the savonius turbine is part of the subcategory of vertical axis wind turbines. The Savonius type turbine, presented for the first time in 1931 by Sigurd J. Savonius [34], consists of a cylinder split in half and moving one part of the other, obtaining as a result a kind of S [35], as observed in Figure 3. The operation of this turbine is based on the use of the drag force generated by the wind on the blades and makes them rotate, so that the torque is generated on the shaft. The drag force must be greater when going in favor than when going against the wind, forward and backward respectively. However, there are certain advantages in Savonius turbines over other vertical axis turbines: their design is quite simple, it presents a good balance between efficiency and facility of maintenance and manufacture [36]. Due to its geometry, the structural resistance of the material in which it is manufactured does not limit its performance [37], in addition its starting capacity and low noise emission make it a good option for urban applications [38].

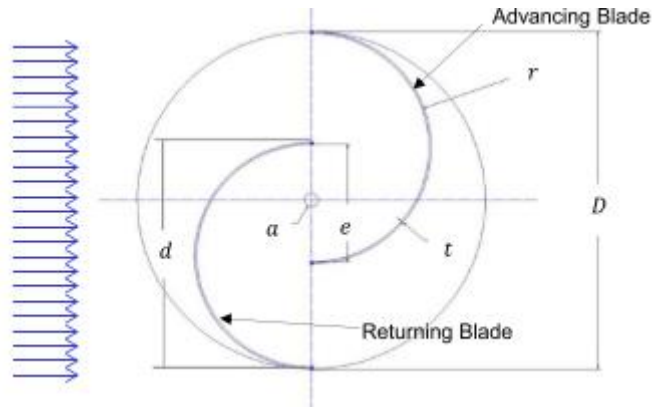


Figure 3 Conventional Savonius Turbine [34]

1.5.1 GEOMETRIC PARAMETERS OF THE ROTOR

To establish the parameters of the rotor design, it is important to define the geometric parameters of the rotor, as well as certain relationships that exist between them. The most important parameters are its diameter and height (D and H , respectively), with which it is possible to calculate the front area of the rotor (A), which is necessary to give an idea of the size of the rotor, and to establish dimensionless coefficients representing its performance of this. This is the area of the rotor that faces the wind flow directly:

$$A = DH$$

There are other secondary parameters such as the diameter of the end plates (D_o), which is slightly greater than the diameter of the rotor, and the diameter of the rotor shaft (a). However, not all rotors have this shaft, there are designs that allow it to be dispensed with.

Another important parameter is the overlap (e), the diameter section in which the two blades (in the case of a two-bladed Savonius) superpose. Figure 4 shows more clearly how overlap is defined, in addition to showing the other parameters that have been defined so far.

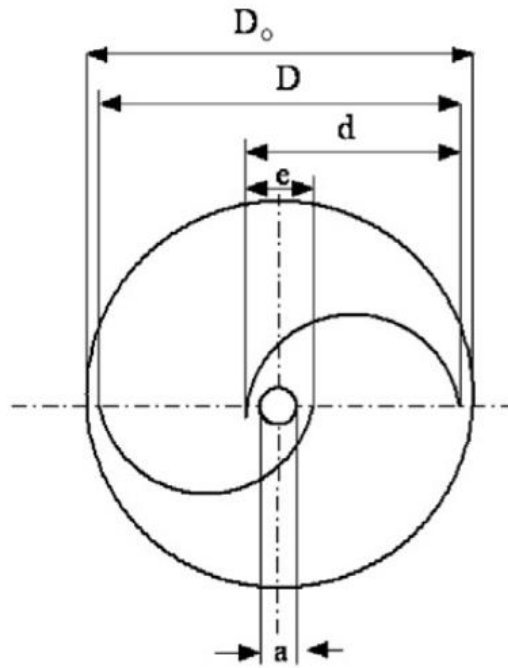


Figure 4 Geometric Parameters of a Savonius rotor [16].

The main relationships between the geometric parameters are the aspect ratio and the overlap ratio. Both have some effect on the performance of this one.

The aspect ratio (α) quantifies the slenderness of the rotor in a dimensionless way, and is defined as the relationship between its height and its diameter:

$$\alpha = \frac{H}{D}$$

Alternatively, it can be calculated as:

$$\alpha = \frac{H^2}{A}$$

The overlap relation (β) is a dimensionless parameter that represents the overlap as a fraction of the diameter:

$$\beta = \frac{e}{D}$$

1.5.2 PERFORMANCE PARAMETERS OF A SAVONIUS TURBINE

In order to be able to compare turbines of different sizes and configurations, dimensionless parameters are established, these parameters represent the main indicators of turbine performance such as torque (T) and power (P).

The power coefficient (C_p) [39], is established as the relationship between the real power developed by the rotor (P), and the power available in the air that passes through a certain area A , equivalent to the projected area of the rotor, as shown earlier. This available power (P_{av}) equals the rate at which kinetic energy passes through that area.

The rate of kinetic energy of a mass of air moving at a certain speed is:

$$P_{av} = \frac{1}{2} \dot{m} V^2$$

Where \dot{m} is the mass flow, the rate at which a unit mass of air passes through a certain cross-sectional area (in this case, this area is equal to the projected area of the rotor); and V is the wind speed.

This mass flow can be expressed as:

$$\dot{m} = \rho AV$$

Where ρ is the density of air. In this way, the energy available in an air mass moving at a certain speed can be expressed as:

$$P_{av} = \frac{1}{2} \rho V^3 A$$

In this way, remembering the power coefficient as the real power developed by the rotor, and the power available in the air, it is established as:

$$C_p = \frac{P}{P_{av}}$$

$$C_p = \frac{P}{\frac{1}{2} \rho V^3 A}$$

It can be rewritten in terms of diameter and height and rearranging the terms:

$$C_p = \frac{2P}{\rho V^3 DH}$$

The torque coefficient (C_t) is established as the relationship between the torque generated in the turbine and the torque available in the moving air, which can be interpreted as a reference torque. Available torque is the product of a force and a distance. This force is established as the exerted by the dynamic pressure of the moving air in the projected area of the rotor. Taking into account that the exerted force by a pressure in an area is simply the product between this pressure and area:

$$F = P_{\infty}A$$

Where P_{∞} is the dynamic air pressure, defined as:

$$P_{\infty} = \frac{1}{2}\rho V^2$$

The distance used to calculate this reference torque is the radius of the rotor, which is reasonable because this is the distance between the axis of rotation and the tip of the rotor. In this way, the reference torque is set as:

$$T_{av} = \frac{1}{2}\rho V^2 Ar$$

Which can be rewritten as follows:

$$T_{av} = \frac{1}{4}\rho V^2 AD$$

And taking into account that $A = DH$:

$$T_{av} = \frac{1}{4}\rho V^2 D^2 H$$

Remembering the torque coefficient as the relationship between the torque generated in the rotor, and the torque available in the air:

$$C_t = \frac{T}{T_{av}}$$

$$C_t = \frac{T}{\frac{1}{2}\rho V^2 Ar}$$

Or alternatively:

$$C_t = \frac{4T}{\rho V^2 D^2 H}$$

Now there are 2 dimensionless parameters that represent rotor torque and power, the main performance parameters that are independent of the rotor size.

The tip speed ratio, λ is a dimensionless indicator that relates the tangential speed at the tip of the rotor (which ultimately represents the rotational speed of the rotor) and the wind speed. The combination of rotational and tangential speed represents the rotor operating condition; the tip speed ratio is the parameter that generally represents the operating condition of a rotor:

$$\lambda = \frac{\omega r}{V}$$

Where ω is the rotational speed.

Having defined the tip speed ratio, it is possible to find a relation between the torque and power coefficients. Recalling that the rotor power can be written as the product of torque and angular velocity:

$$P = T\omega$$

Carrying out the relation between power coefficient and torque:

$$\frac{C_p}{C_t} = \frac{T\omega \frac{1}{2}\rho V^2 Ar}{T \frac{1}{2}\rho V^3 A}$$

Thus

$$\frac{C_p}{C_t} = \frac{\omega r}{V}$$

Finally

$$C_p = \lambda C_t$$

This expression allows to easily calculate one coefficient from the other.

In general, the performance of a turbine is characterized by means of a curve that specifies the power coefficients for a range of λ , thus representing the performance of the rotor for a complete range of operating conditions; that are, various combinations of wind speed and rotational speed.

The torque varies with the position of the rotor in relation to the direction of the wind. In each revolution, this reaches its maximum and minimum value, with the maximum around 90° between the rotor and the wind (with the wind affecting the all the rotor), and the minimum around 0° (in rotors with two blades). With this, it can be calculated the work done in each revolution and thus, the estimate average rotor power.

1.5.3 PERFORMANCE IMPROVEMENT OF THE SAVONIUS TURBINE

The performance of a turbine is usually determined by a dimensionless variable called the power coefficient; the power coefficient is a variable that relates the amount of energy that a turbine extracts with respect to the amount of energy available in an area. Although Savonius turbines have a low power coefficient, as shown in Figure 5, they stand out for being turbines with good performance at low speeds, easy to manufacture and with high independence from the wind direction. For this reason, many researchers have conducted studies to improve the efficiency of these turbines. A simple but proven alternative is to optimize the geometry of the rotor profile in a way that improves efficiency without increasing the complexity of the system. Some studies present the Bach profiles as the ones with the best performance, because they are the ones with the best lift and drag characteristics for this type of application [29], [40]. However, more recent optimizations of the geometry have been carried out, coinciding in profiles whose curvature peak is around $2/3$ of the radius, despite the fact that the parameterization of the profile geometry is carried out in different ways. Other studies have parameterized the curve with different points of a cubic spline [41] [42], while other authors have reached similar geometries defining the profile as a segment of an inclined ellipse [43] [44]. These types of geometries improve efficiency by up to 33%, coinciding with a TSR of 0.8. Another proposal regarding the variation of the profiles is the use of aerodynamic profiles in the rotor to try to take advantage of its ability to generate lift. The study of the different profiles does not find advantages in the use of aerodynamic profiles for the blades of a Savonius rotor [29], however a more recent work manages to improve the efficiency of a Savonius rotor using aerodynamic profiles of high curvature [20].

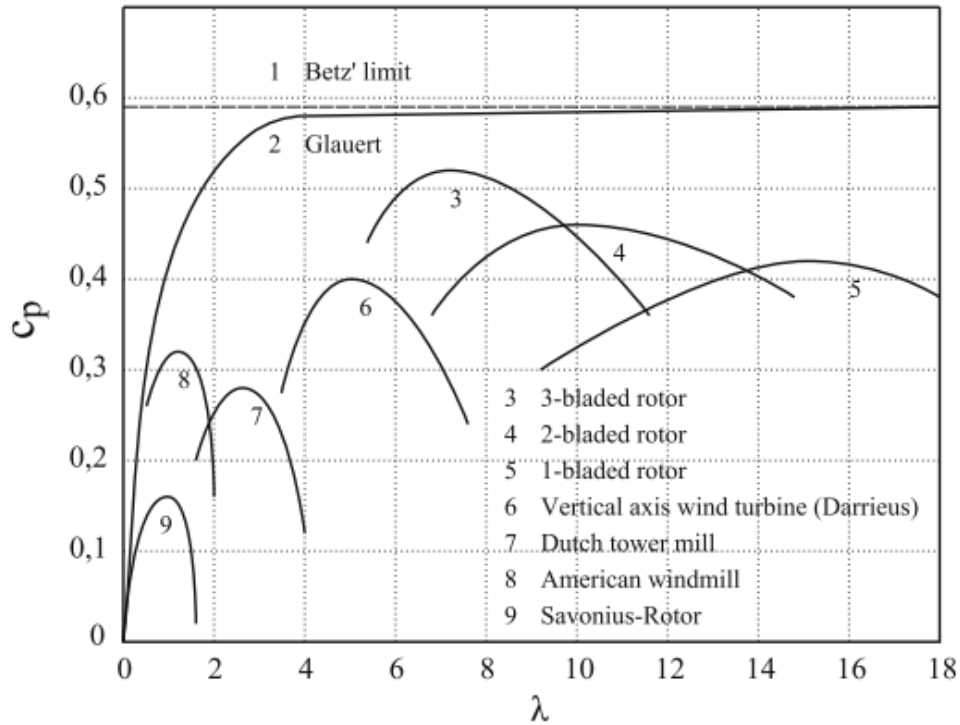


Figure 5 Power coefficient curves for wind turbines [33]

On the other hand, a lot of use has recently been made of optimization tools such as genetic algorithms or particle swarm optimization [19], [38], [41], [43], [45] to obtain relatively simple designs that are quite better than a Savonius rotor with a semi-circular profile.

1.5.4 SAVONIUS ROTORS OF VARIABLE GEOMETRY

As an alternative for improving the performance of variable geometry Savonius rotor while maintaining their independence from the wind direction, studies have been carried out on the feasibility of rotor blades with variable geometry. One of the first proposals for a Savonius with variable geometry rotor was made in 1982 [46], when it was proposed to manufacture the rotor blades in fabric. One of the main advantages of this type of Savonius rotors would be their low weight, but it was mainly expected that the change in the shape of the blades when it goes forward and backward would improve the performance of the rotor. The advancing blade inflates due to the wind entering it from the front, thus increasing drag; while when the blade moves back, its shape contracts due to the flexibility of the fabric, thus reducing drag. This cyclical deformation would be beneficial to the performance of the rotor, not to mention the advantage of its low weight. Initially the studies showed an improvement in the performance of fabric blades, as long as the fabric remains warm. Attempts were made to take advantage of the flexibility of the fabric to make the blade geometry convenient to control. By means of vertical bars joined by the fabric, a modifiable profile could be created while rotating; however, initially there were not very good results due to the complexity of the shape change mechanism. The friction in this consumed the additional energy that could be obtained thanks to the designed geometric variations [47].

Recently, the study of these fabric rotors has been studied in depth. Ghosh et. [48] carry out experimental tests of fabric rotors, among which a Savonius is tested; one of the main advantages mentioned is its low cost and ease of manufacture. However, tests show that Savonius type with fabric rotors do not show an improvement over conventional Savonius. The low power coefficients achieved by this type of rotors are associated with the porosity of the material with which they are built, so the feasibility of implementing this type of rotors is not completely discarded. A novel modification is studied by Ersoy et. [49]. The modification consists of adding an extension of fabric (deformable) to the blades of a conventional Savonius rotor. The performance characteristics of the motor are improved with respect to the conventional Savonius rotor; the rotor is able to start at lower speeds and the energy production is higher. This is achieved with an increase in manufacturing and maintenance costs of no more than 10%.

Slightly more advanced and novel alternatives have been proposed thanks to the availability of CFD software that allow fluid-structure simulations to be performed that allow the prediction of aerodynamic loads at the same time as deformations of the rotor geometry, which in turn generate changes in the same aerodynamic loads. The process of these complex designs is considerably lightened by advances in optimization methods. Marinić-Kragić et. [45] propose a design methodology for a flexible Savonius rotor. The initial geometry of the rotor is obtained with the help of a genetic algorithm, through which it is possible to improve the efficiency of a base rotor by 18%. This rotor design allows the blades to deflect passively by aerodynamic and inertial forces as they rotate and interact with the flow. The deformation of the blades is allowed as far as their structural restrictions allow, obtaining an additional 8% increase in rotor performance. Blade deformation is not actively controlled. It is found that at higher operating TSR, the increase in efficiency due to the deformation of the profile is even greater, thus obtaining a versatile design. However, this type of rotors is limited by the structural constraints of the material; the design by means of genetic algorithms fed by CFD simulations can have a high computational cost and the simulations that take into account the fluid-structure dynamic interaction are more complex to prepare, in addition to their higher computational cost.

Much more promising results have been achieved with deformable rotor designs such as the one proposed by Sobczak [50], reaching efficiencies of 0.39, in increase of around 90% compared to the performance of a conventional Savonius rotor as a reference. The deformation of these blades occurs from the center of the rotor, where the two blades meet, leaving their tips fixed. A deformation is actively induced in the geometry of the profile during the entire rotation of the profile, so that the advancing blade increases its area exposed to the flow (in turn increasing drag), while the receding blade reduces its area, also reducing drag. This allows the forward blade to generate more positive torque, while the backward blade generates less negative torque; greatly increasing efficiency. The working principle is shown graphically in Figure 6.

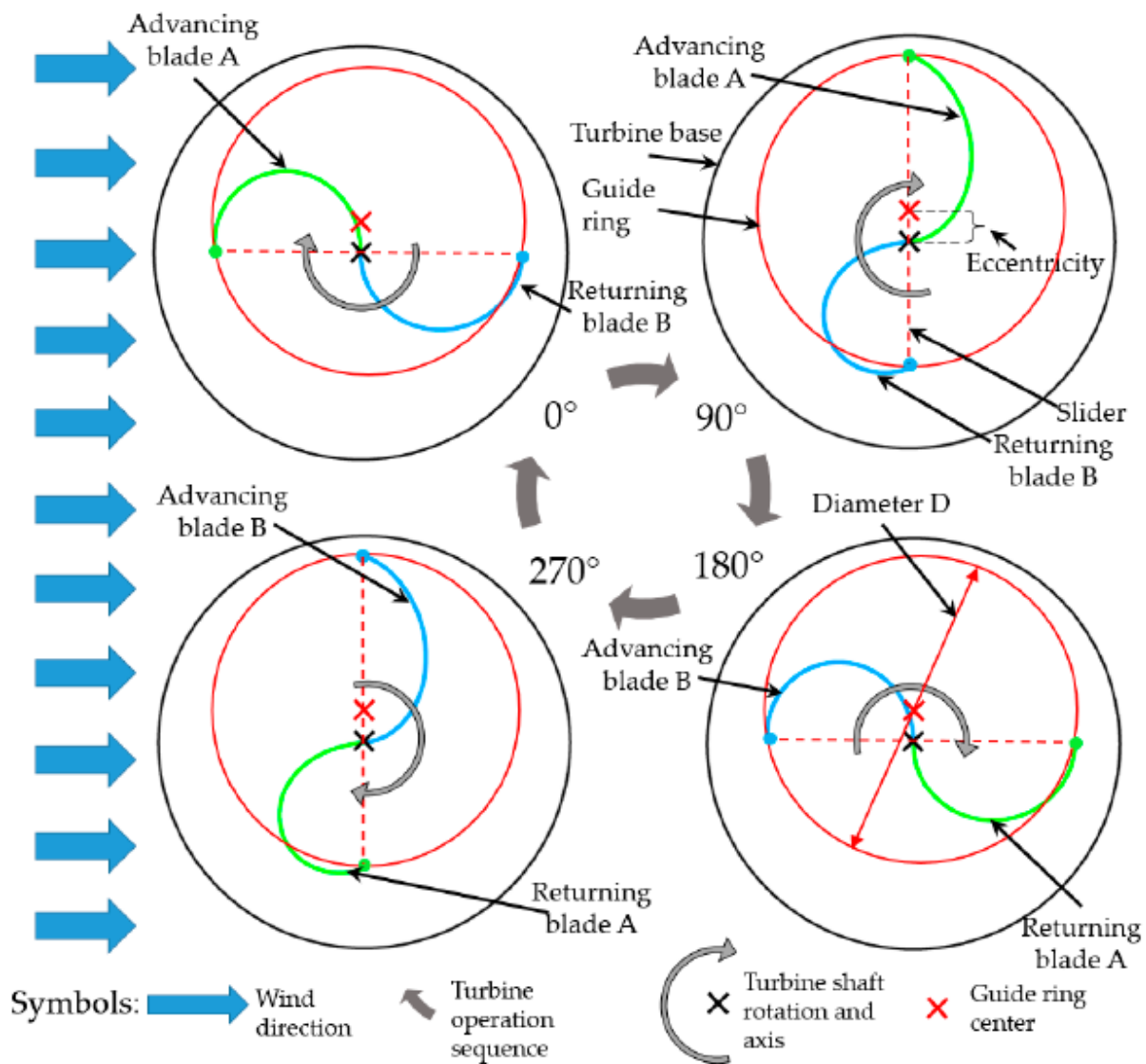


Figure 6 Rotor working principle proposed by Sobczak [50]

It is concluded that a greater deformation of the profile increases its performance more, however, so far no experimental tests have been carried out, and it is very likely that the mechanism to induce the required deformation in the material is quite complex, in addition, the consume part of the energy that is generated in the rotor. The fatigue resistance of the material is another matter that requires considerable attention in this proposal; the susceptibility to fatigue of this type of rotor could increase the maintenance costs.

1.5.5 SIMULATION OF SAVONIUS TURBINES

The evaluation of this type of wind turbines that work with drag is somewhat more complex than the generators that work with lift. There are relatively simple methods that allow estimating the performance of horizontal axis wind turbines, such as the Blade Element Momentum Theory (BEM) [51]. Through this method it is possible to estimate performance parameters such as torque, power

and thrust generated by the rotor under certain conditions. The results are good as long as the data provide to the method is reliable. There are also methods such as the single and multiple stream tube method [52], [53], which allow the analysis of vertical axis turbines whose operating principle is lift, such as Darrieus type turbines. Methods such as Reynolds-averaged Navier-Stokes Equations (RANS), or Large Eddy Simulations (LES) are much more robust methods, in which much more details of the phenomena present in the rotors are taken into account, such as the effects on the tips of the rotors blades, their interaction and turbulence [54]. These methods can be implemented in computational fluid dynamics (CFD) such as Fluent module of the software ANSYS; which allows the simulation of any type of rotor; its precision is greater, however, the computation time required for this type of simulation is higher.

For Savonius rotors there is not a simple reliable method to be used in the design of one of these. The only reliable option left is CFD simulations. Many studies on the performance of this type of rotors have been carried out by means of this type of simulation [52], [54] - [60]. These simulations also allow simulating the behavior of the rotor in a transient state [57], observing the behavior of the flow throughout the entire geometry, and evaluating different variations to the rotor design such as inlet ducts [56], [58] , flexibility in the blades [12], [54], etc.

Two-dimensional simulations can be performed, in which only the geometry of the blade profile is taken into account, with the interaction between them, and between them and the flow. It is a type of simplified simulation that is very useful as a first approach to the design of rotor profiles. These simulations are relatively fast compared to three-dimensional simulations, but they do not take certain phenomena into account, so they are less reliable. This is why they are used in preliminary profile design stages, in which different variations in profile geometry may be evaluated and require a considerable number of simulations.

In this type of simulations, there is a rotational subdomain that encloses the geometry of the profiles, and an outer stationary domain, as shown in Figure 7. The rotational subdomain allows capturing the effects of the rotation of the profiles. It is important to establish the interface between these domains to not have problems in the simulations. The rotational subdomain generally has finer elements than the outer domain. The area of the fluid near the profile walls is generally refined to calculate boundary layer effects.

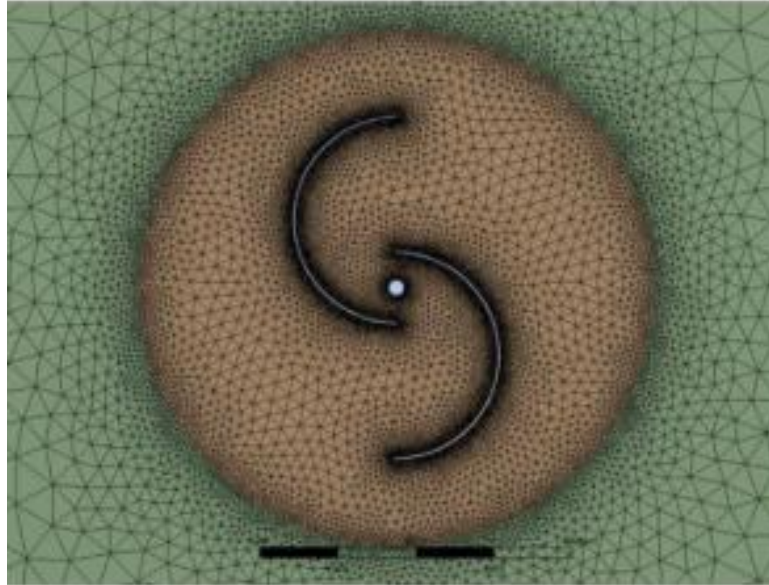


Figure 7 3D mesh with 5 million elements [61]

This geometric model for the simulation of rotors in 2 dimensions has been widely used for the preliminary estimation of performance parameters [5], [40], [44], [58], not only for Savonius rotors, this method is valid for vertical rotors in general, such as the straight-bladed rotor studied in [5]. All the mentioned works coincide in the $k-\omega$ SST turbulence model. This is a model that emerge from the need for better predictions in the aeronautical field [62], the $k-\omega$ SST model predicts the adverse pressure gradients more satisfactorily when compared to other models [63].

To have a more appropriate modeling of the flow behavior around the rotor, it is important to perform three-dimensional simulations. In this type of simulation, it is possible to take into account the interaction of the blades with the rotor end-plates, as well as the deflection of the flow in the vertical direction. In the two-dimensional simulations, it would be assumed that the flow is totally perpendicular to the axis of rotation, when in reality it is deflected in the direction of that axis. Three-dimensional simulations allow these phenomena to be taken into account. Studies such as those carried out by Ferrari [60], Larin [61] or Dobrev [55], in which two-dimensional and three-dimensional simulations are compared, agree that, indeed, the two-dimensional simulations are not sufficiently precise, since they overestimate the performance of the rotor, in addition to not predict accurately the point of maximum rotor efficiency. The results obtained through three-dimensional simulations are close to experimental results using the same turbulence model mentioned above: $k-\omega$ SST. However, in the study by Larin [61] is decide on the $k-\epsilon$ model as the most appropriate. The geometry of this type of simulation follows the same logic as the presented for the two-dimensional simulations. The rotational subdomain is a cylinder that contains the complete geometry of the rotor. This subdomain is itself contained in the foreign domain.

1.5.6 STATISTICAL METHODS

By means of CFD methods such as those mentioned previously, it is possible to estimate the coefficients of performance of the rotor, or to have an estimate of the rate of the energy production under certain conditions, this, at a certain wind speed and a certain rotational speed. However, in

real applications, the wind speed varies, even more considering the type of application for which the Savonius rotor is going to be design: urban areas in which the wind speed varies considerably, and in an unpredictable way.

There are several models by which can be modeled the probability that the wind picks up a certain speed. By means of experimental coefficients, the effects of the terrain are taken into account [51].

One of the best know methods is the Rayleigh probability distribution, which is defined as follows [64]

$$f(V) = \frac{\pi V}{2 V_m^2} \exp \left\{ - \left[\frac{\pi}{4} \left(\frac{V}{V_m} \right)^2 \right] \right\}$$

$f(V)$ represents the fraction of time that the wind has velocity V . The Rayleigh probability distribution is a simplified version of the Weibull one. It is a specific case in which the factor form is assumed with a value of 2.

With the Rayleigh probability distribution, it is also possible to model the probability that the wind speed takes values in a certain range:

$$P(V_1 < V < V_2) = \exp \left\{ - \left[\frac{\pi}{4} \left(\frac{V_1}{V_m} \right)^2 \right] \right\} - \exp \left\{ - \left[\frac{\pi}{4} \left(\frac{V_2}{V_m} \right)^2 \right] \right\}$$

The Weibull probability distribution model may be a bit more precise, but it requires knowing certain data about the terrain in which the wind probability is going to be modeled. This may be a better alternative as long as the information is available. Weibull distribution has the following form [65]:

$$f(V) = \frac{k}{V_m} \left(\frac{V}{V_m} \right)^{k-1} \exp \left[- \left(\frac{V}{V_m} \right)^k \right]$$

Now, the probability that the wind speed takes values within a certain range, according to the Weibull distribution, is:

$$P(V_1 < V < V_2) = \exp \left[- \left(\frac{V_1}{V_m} \right)^k \right] - \exp \left[- \left(\frac{V_2}{V_m} \right)^k \right]$$

Both the scale factor, equivalent to the average speed in the area (V_m), and the form factor (k), can be found in wind atlases such as the European Wind Atlas [66].

These are the most common distributions; however, different variations and combinations have been studied between different probability distributions such as bimodal Weibull, truncated normal Weibull, Gamma-Weibull, etc. [67].

1.6 EQUIPMENT FOR AUTOMATION

Some actuators, sensors, and microcontrollers used for system automation will be mentioned in the next chapter. Some items that can be used to propose solutions for changing blades for the Savonius turbine will be presented.

1.6.1 ACTUATORS

Actuators are devices that transform hydraulic, pneumatic or electrical energy in order to generate a force so it can generate a change in position. They have other functions, but the focus will be the change of position. Actuators are divided into two groups by the type of movement they generate: linear and rotary. Also, they are divided by the type of energy used: pneumatic, hydraulic and electric.

Pneumatic actuators are those that use compressed air to generate movement. They use the air inside a closed container to be compressed and with this generated pressure, the necessary force to carry out the movement is produced. These actuators generate a precise linear motion, providing accuracy.

Hydraulic actuators have the same operation as pneumatic, but the difference is that they use pressurized fluids. They are widely used for their power / weight ratio which serves to move or deform heavy objects, although they require too much equipment to supply this power.

Electric actuators transform electrical energy into movement, they are the most used since their power source is electrical energy and they do not require compressors such as hydraulic and pneumatic. These use the electromagnetic force to generate a displacement which produces the force [68].

1.6.2 MICROCONTROLLERS

A microcontroller is an integrated circuit which can be programmed to perform various tasks. It could be said that they are microcomputers since they have the same components: a central processing unit, memory and input / output resources to communicate with other devices. One of the best known is the Arduino [69].

In the ambit of microcontrollers Arduino is one of the most used. Is like a small device that works like a computer, it is known as a physical or embedded computing platform that can interact with

other systems through the use of hardware and software. Its behavior is controlled by means of algorithms in C / C ++ language and through wires or other connections it will give and receive commands in order to perform a specific task [70].

Other microcontroller that is widely use is the Raspberry Pi, this microcontroller mostly uses because it supports the world most use programming language: Python. This microcontroller has the more powerful processor and a maximum RAM of 8 GB, which means is faster and can support large amount of data. Also, it has micro-HDMI and USB ports that can be used to connect it to other devices, this is commonly use with screens because the Raspberry Pi is a tiny computer. Its disadvantages are its price, because of its processor and memory. Also is harder to use, and because of its complexity, is mostly use in complex projects so is not good option for less complex projects [71]

1.6.3 SENSORS

Sensors are electronic devices that use electricity to generate a measurement according to the physical magnitude that needs to be measure or study. It can be length, weight, speed, etc. These devices generate an electrical signal which is converted to another signal from which the measurement of the physical magnitude is extracted. Clearly depending on the type of sensor, these signals are extracted and converted differently [72].

2. METHODOLOGY

2.1 ROTOR DESIGN

The idea is to design a Savonius rotor whose geometry variation to different operating conditions makes power generation more efficient, taking into account that the rotor's application is urban and the winds are unpredictable in this type of environment.

For these urban applications, the turbines are typically small. Big energy demands are supplied by large wind farms located far from the urban area; additionally, in urban areas there are not very large spaces available. This is taken into account for the dimensioning of the rotor to be designed. It can be set the diameter of this, taking into account the typical values for the aspect ratio of the rotor.

A rotor height of 60 cm is selected, taking into account size restrictions. The aspect ratio has an effect on the performance of the rotor, as shown in different studies [11], [44], [73], however, there has been a considerable difference in what is the optimal value of aspect ratio in this type of rotors. Neither has a trend been defined with respect to this geometric parameter, although, a relationship between its optimal value and the other rotor parameters, such as overlap, number of stages, or profile geometry has been evidenced.

Studies such as the one realized by V. J. Modi et. al [44], in which wind tunnel tests are carried out on Savonius rotors with different geometries, it is found that an aspect ratio of 0.77 maximizes efficiency. A study realized more recently by MA Kamoji, in which the influence of different geometric parameters on the performance of Savonius rotors is similarly studied by means of wind tunnel tests, finding optimal values of the ratio with similar appearance, ranging between 0.64 and 0.7. This would indicate that it is desirable that the design of this type of rotors have a relatively low aspect ratio. However, other studies suggest that high aspect ratios improve rotor performance, limited by structural design limitations [73]. In this series of experiments, the rotor with the highest aspect ratio (4.8) performed better in terms of performance. According to [11], typical values for the aspect ratio of a Savonius rotor are between 1.5 and 2; values in which, generally a good performance is obtained. Figure 8 shows the performance of rotors with aspect ratios between 0.5 and 5, showing how slimmer rotors managed to achieve higher performance overall. The difference between the rotors with aspect ratios 2, 4 and 5 is not very considerable, so it can be said that as the aspect ratio of the rotor is increased, the positive effect of this decreases.

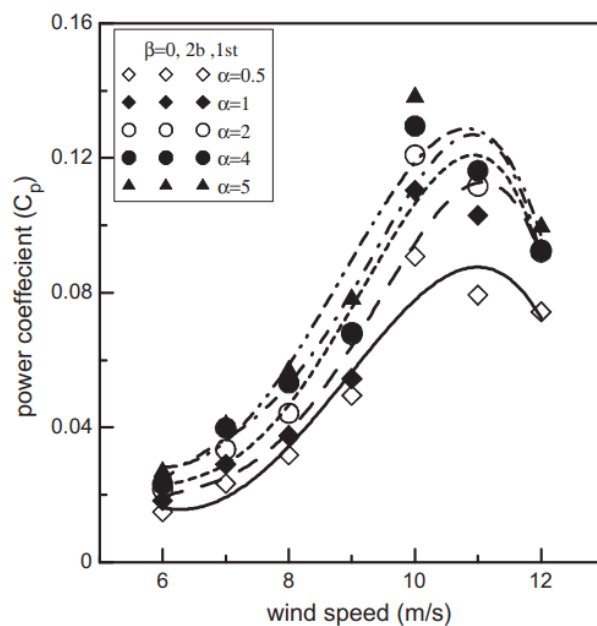


Figure 8 Effect of aspect ratio on the performance of a Savonius rotor [74]

Taking the previous into account, an aspect ratio of 1.67 is selected for a diameter of 36 cm. With this, an area of 0.216 m² is obtained.

The overlap in this type of rotors allows a convenient interaction of the flow in both rotor blades. Taking into account that overlap can have positive effects on rotor performance, an overlap ratio of 15% is chosen for this case, as suggested in [13], where it is concluded, after a numerical analysis, that this is a suitable value for Savonius rotors, presenting a good performance for a wide range of operating speeds. It is then, an overlap of 5.4 cm.

Now the main geometric parameters of the rotor have been defined. Table 1 shows a summary of these.

Table 1 – Geometric parameters of the rotor. Own elaboration

Diámetro (cm)	36
Altura (cm)	60
Área (cm²)	2160
Overlap (cm)	5.4
Relación de aspecto	1.67
Relación de overlap	0.15

There is no central axis because the end plates allow it to be discarded.

2.1.1 PROFILE SELECTION

To define the different shapes of the profiles, a study of different geometries is carried out, and how variations in these affect the performance of the rotor. The parameterization of the geometry is done by means of a spline with 5 control points. The first two and the last two points are fixed, and the third one is left mobile in the 2 axes to vary its location and with this the shape of the profile. The X and Y coordinates of this movable control point are measured with the origin located in the center of the rotor shown in Figure 9. The X axis goes to the left and the Y axis goes up, and the control point is located in the rotor blade that is located on the positive Y axis.

The 2-D simulations are carried out to evaluate the different generated profiles, this type of simulation is suitable for comparing profiles, 3-D simulations would require much more time. The objective is to obtain different geometries for 3 different speed regimes, taking into account the operating range of this type of turbines; in this way, profile designs for speeds of 3 m / s, 6 m / s and 10 m / s are obtained. To define the rotational speed at each of these operating conditions, a TSR relationship of 0.8 is established. This value is chosen because in several works it is evidenced that this is the value at which the maximum power is generally obtained in Savonius rotors [43], [44], [75]; the way to keep this TSR constant is through the generator that is connected to the rotor shaft.

2.1.2 SIMULATION 2D

A type C mesh is used, similar to that used for aircraft profile simulations. Around the rotor profile there is a rotational domain, as shown in Figure 9. The external part of the mesh is made as structured as possible in order to capture better the effects of rotation. The section of the mesh that captures the wake of the rotor, in addition to its surface, is refined in order to capture the effects of the boundary layer, as shown in Figure 10.

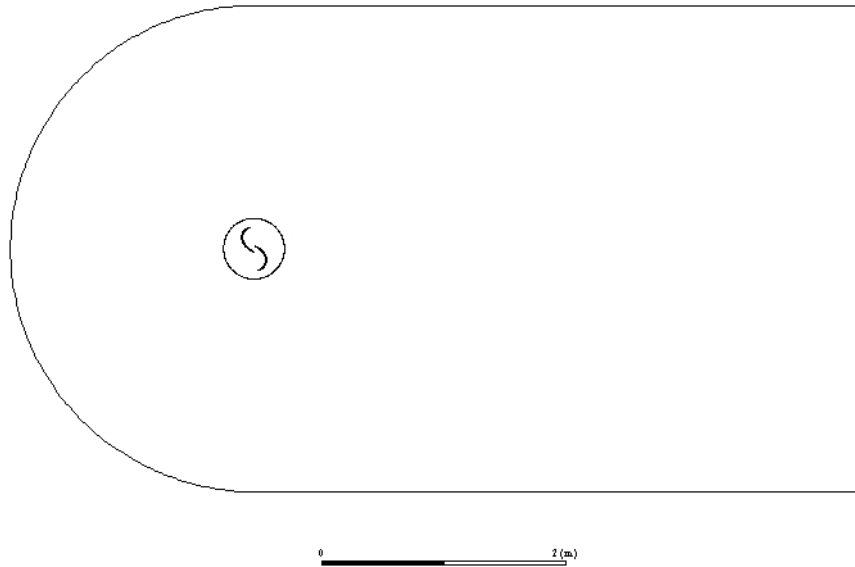


Figure 9 Geometry for profile simulations. Own elaboration

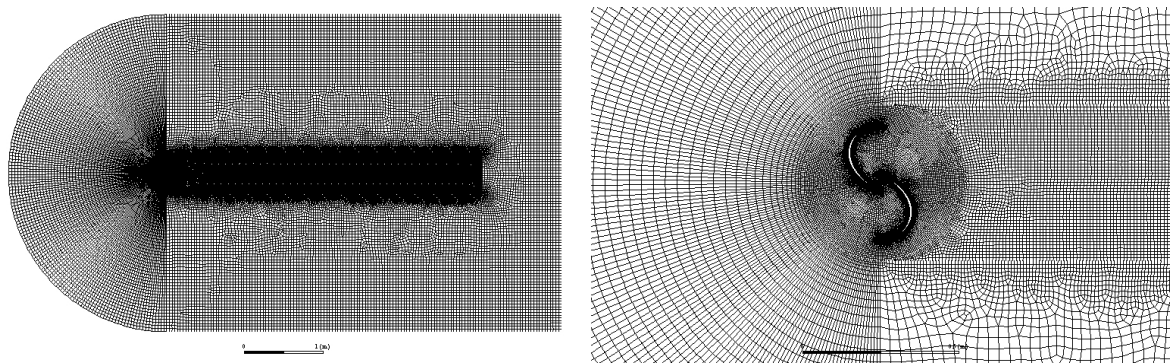


Figure 10 General (left) and detailed (right) views of the mesh for profile simulations. Own elaboration

In order to obtain reliable results, a mesh study is carried out, this consists of increasing the number of elements and seeing the behavior of the observed variable, in this case the torque, when the relative error varies less than 3% it can be said that the mesh will not significantly affect the result. This study is important because an optimal mesh can considerably improve the efficiency of the optimization process. Six different meshes are compared, which their characteristics are shown in Table 2. The error is calculated with respect to the finest mesh. In this way mesh No. 3 is selected, being the thickest mesh with a very reasonable error obtained (1.10%). The size of the elements in the 6 meshes is kept constant in the section of the profile surface taking into account the thickness of the boundary layer.

Table 2 – Mesh independence study

Thin	Medium	Gross
------	--------	-------

	1	2	3	4	5	6
Base size (m)	0.2	0.4	0.7	1.0	1.2	1.5
No. Elements	125708	138945	155480	213524	434565	1340222
Torque (N m)	1.1606	1.1471	1.1480	1.0732	1.0903	1.0677
Error	--	1.18%	1.10%	8.14%	6.45%	8.70%

Having selected the mesh and having defined the way in which the different geometries will be studied, the selection of the profiles for each speed is carried out, taking into account the results of the 2D simulations. After evaluating 17 different profiles for each of the speeds, 2 different geometries are obtained. Geometry 1 (see Figure 11) turned out to be the most suitable profile for the turbine when operating at low speeds (3 m / s) while for higher speeds (between 6 and 10 m / s) it was with a single geometry (Geometry 2, as shown in Figure 11) that the best performance was obtained.

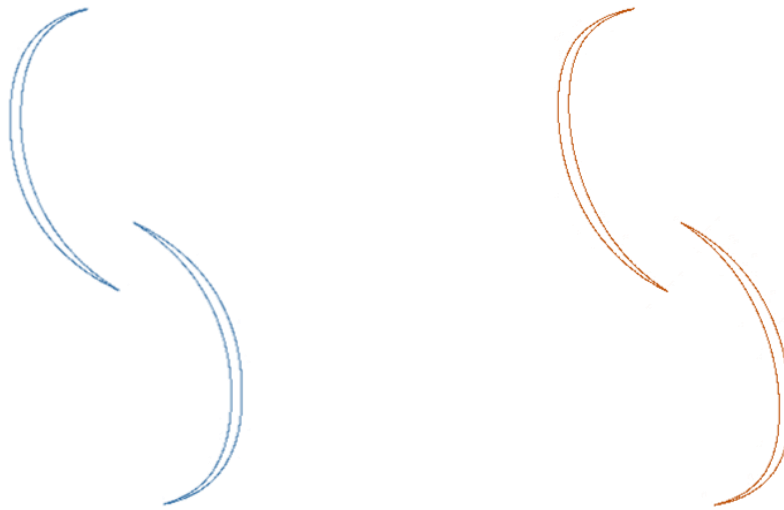


Figure 11 Geometries 1 (blue) and 2 (orange). Own elaboration

Table 3 shows the results for the first 9 profiles evaluated; from these nine profiles a single suitable profile was found for the 3 selected speed regimes. A series of simulations is carried out varying the geometry of this profile in a slighter way, finding a different geometry than the previous one that behaves better at 3 m / s, the results are shown in Table 4. Thus, a rotor is obtained whose geometry adapts to 2 different speed regimes, obtaining the extraction of energy in the most efficient way possible at those 2 regimes.

Table 3 – Characteristics of the first 9 evaluated profiles

Geometry				Power Coefficient		
Coord	X	Coord	Y	3 m/s	6 m/s	10 m/s
(m)		(m)				
0.1		0.05		0.193	0.201	0.199

0.1	0.1	<u>0.197</u>	<u>0.209</u>	<u>0.205</u>
0.1	0.15	0.181	0.191	0.190
0.18	0.05	0.181	0.187	0.185
0.18	0.1	0.180	0.188	0.179
0.18	0.15	0.167	0.177	0.178
0.27	0.05	0.102	0.110	0.107
0.27	0.1	0.070	0.081	0.082
0.27	0.15	0.034	0.048	0.039

Table 4 – Characteristics of the profiles evaluated with smaller variations in geometry

Geometry		Power Coefficient		
Coord X (m)	Coord Y (m)	3 m/s	6 m/s	10 m/s
0.06	0.08	0.175	0.188	0.186
0.06	0.1	0.169	0.184	0.183
0.06	0.12	0.163	0.179	0.180
0.1	0.08	<u>0.201</u>	0.204	0.200
0.1	0.1	0.197	<u>0.209</u>	<u>0.205</u>
0.1	0.12	0.194	0.204	0.202
0.14	0.08	0.196	0.203	0.200
0.14	0.1	0.199	0.207	0.203
0.14	0.12	0.196	0.206	0.201

2.1.3 3D SIMULATION

To evaluate the final geometry, 3D simulations are necessary in order to capture the effects that are presented in the rotor tips, in addition to the drag of the plates. For these simulations, a type C mesh is also made with 1'081,205 elements. To be sure of having correct results when evaluating the performance of the final geometry, a simulation of a rotor is carried out for which there are experimental results in a wind tunnel, as well as information about its geometry. The rotor tested by Ali in [75], is a conventional Savonius, without overlap and semicircular profiles; with a total diameter of 20 cm and a height of 20 cm. In the work, the power curve is reported at different TSR, varying speeds between 3 m / s and 6 m / s, a speed regime that is very similar to that used for the design of this work. The experimental results were obtained in a wind tunnel, but were not corrected for the effects of the tunnel walls on the rotor. Therefore, before comparing the experimental results with those obtained by means of CFD, they are corrected according to the methodology presented by Roy in [76]; this methodology applied specifically to Savonius rotors, corrects the speed at which the tests must be performed. A specific speed in the tunnel corresponds to a slightly lower speed when the rotor is in operation; higher values for power are obtained in the tunnel compared to those actually obtained in practice. Comparing the corrected experimental results with the CFD simulations of the same rotor (see Figure 12), an error of around 14% is found,

an acceptable deviation that indicates that the mesh and the model being used are correct to evaluate the rotor of variable geometry design.

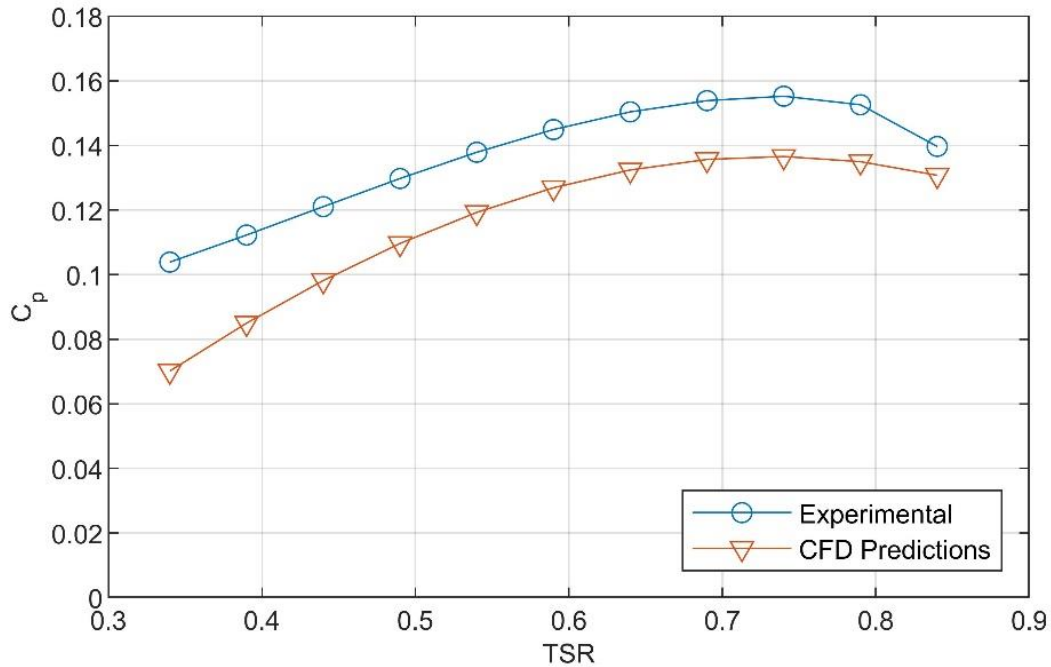


Figure 12 Comparison of the experimental power curves and those obtained by means of CFD [76].

2.1.4 GEOMETRIC DETAILS OF THE ROTOR

In previous sections the details of the geometries of the profile for the different speeds are shown, besides mentioning the measurements of the endplates, height and rotor diameter. Figure 13 shows the 3 views and the isometric of the rotor with its main dimensions. The profile seen in the isometric is the profile selected for high speeds (6 and 10 m / s, see Figure 11). An additional plane is not shown for the other geometry because the measurements specified in Figure 13 do not change with the variation of the profile.

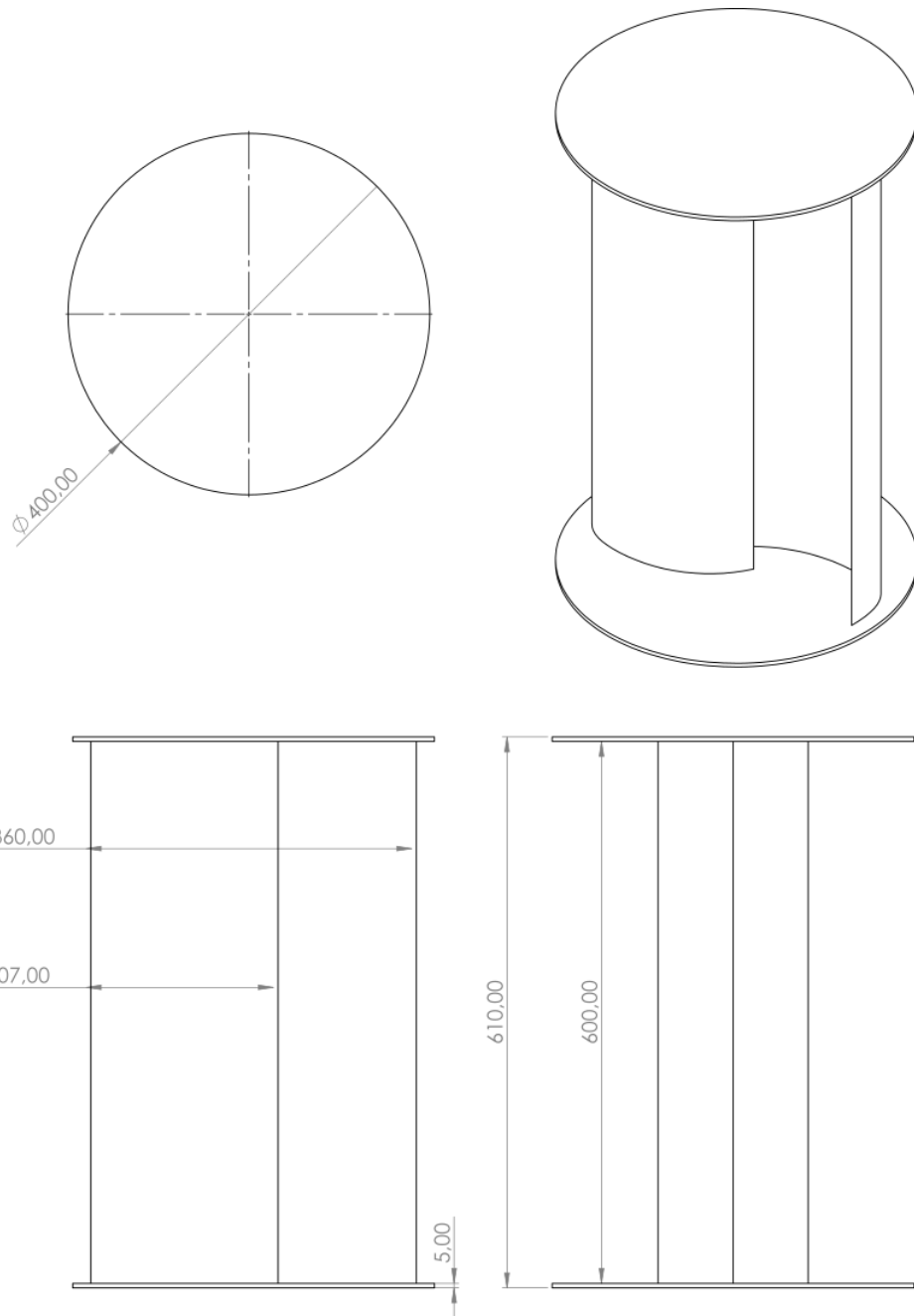


Figure 13 - Other geometric details of the rotor.

For solution 3 there is a change in the blades, but the dimensions remain the same

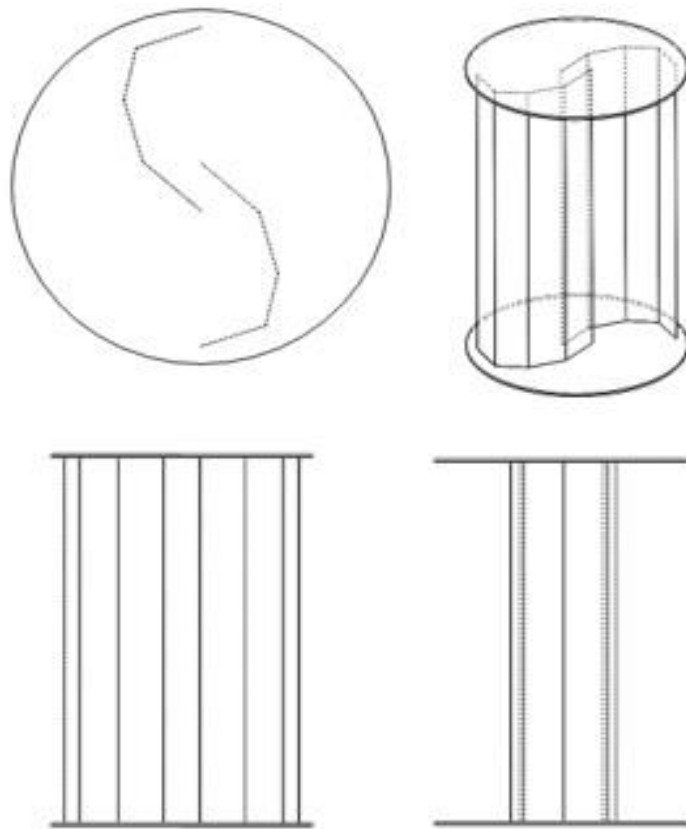


Figure 14- Geometric details of the rotor for solution 3

2.1.5 OPTIONS TO CHANGE THE TURBINE GEOMETRY

For the turbine change system designs, 3 solutions are presented, Solid Edge software will be used. The geometries of the blade are semi-ellipses with a major axis and a minor axis, of which 1 pair of semi-ellipses would be of equal measurements, and the other pair with different major and minor axis. For solution 1 and 3, simple geometries will be used that would represent automated instruments.

After the designs, they will be evaluated with a decision matrix that consists of a table where each solution will be presented in the first row, and in the first column each important aspect that is considered for the investigation. The aspects to analyze are: Geometry shape fidelity, estimated cost, drive independence, complexity of the solution and reliability of the solution. Each of these 5 aspects will receive a score between 1 and 5 depending on the solution that is being analyzed, with 1 being the minimum score and 5 the maximum score, so that in the end, take the average of each solution is calculated and then, the highest value will be choose, which would represent the best solution.

3. RESULTS

3.1 SIMULATION 2D RESULTS

With the data generated for the different profile geometries it is possible to establish certain relationships between the geometry and its performance. Figure 15 shows the power coefficients obtained for various X positions of the control point; these values correspond to a Y position of 0.1 m at a speed of 6m / s. Figure 16 shows the power coefficients obtained for various Y positions of the control point; these values correspond to a position in X of 0.18 m at a speed of 6 m / s.

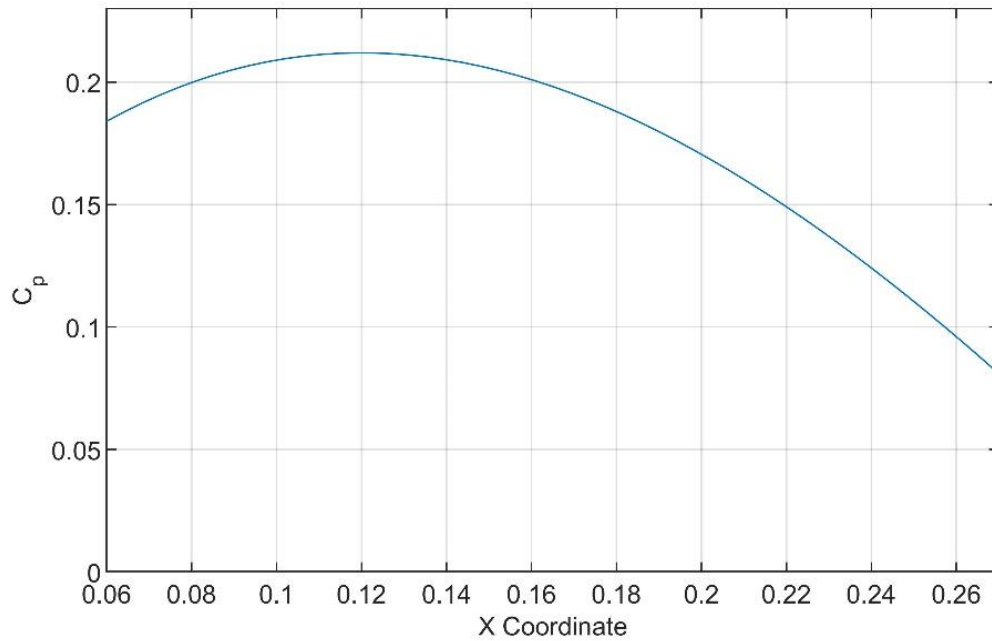


Figure 15 Power coefficient for various X coordinate values of the control point. Own elaboration

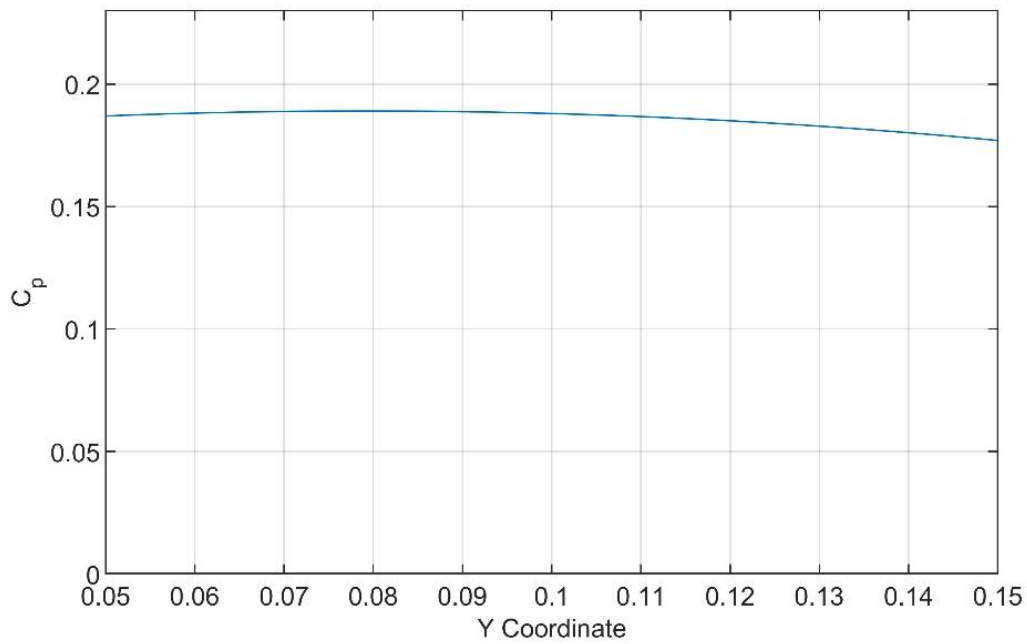


Figure 16 Power coefficient for various values of Y coordinate of the control point

The X coordinate represents the concavity of the profile, while the Y coordinate represents the maximum point of the curvature. According to Figure 15 and Figure 16, it is evident that the performance of the profile is much more sensitive to the concavity of the same, while the point of maximum curvature does not have a very significant effect. A high concave profile can develop more drag, from that, very low concavities are not very efficient, compared to moderate concavities. However, a very high concavity is not very convenient, as shown in Figure 15. This can be associated with the fact that a blade that is too concave is also long, and all this length would be completely exposed to the air flow at the moments of rotation in which one blade just finishes its advance and the other just finishes its recoil, affecting performance considerably.

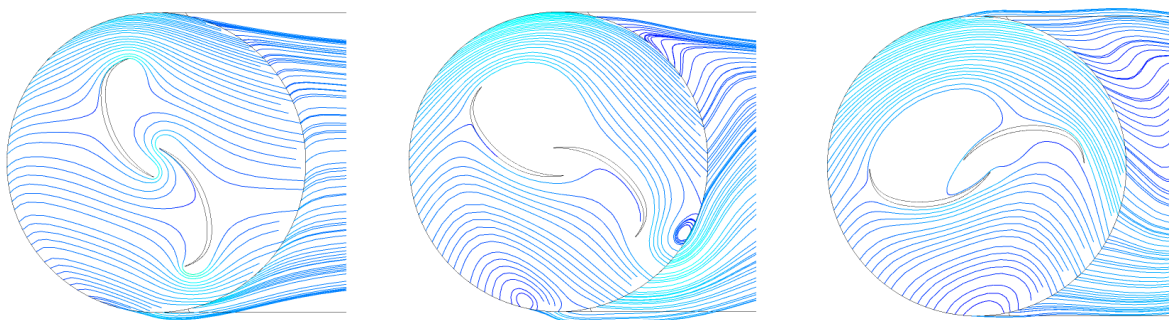


Figure 17 Behavior of the flow in the profile at different points of the rotation (Geometry 2, for a speed of 10 m/s at a TSR of 0.8). Own elaboration

Figure 17 shows the flow behavior in one of the evaluated profiles (Geometry 2), for 3 positions of the rotation. From left to right: facing the flow, at 45 ° and parallel to the flow. With the rotor facing

the flow, it can be seen how the blade that advances (the lower one) leaves a trail of disturbed flow while the trail of the backward blade is somewhat softer. In addition, the effect of overlap is seen, which allows the flow in the lower part of the advancing blade to have a certain interaction with the receding blade, helping in a certain way to overcome the opposition to the backward movement of the same. At the other points of the rotation, where less torque is generated, a more disorderly flow is evident.

Figure 18 shows the pressure distribution in the profile. On the left is the flow in front of the rotor, at the point where the greatest torque is generated. In this case, it can be seen that there is a greater pressure along the entire surface of the advancing blade, and although high pressures are also seen in the receding blade, these occur on a smaller surface, so the force generated on this blade due to pressure is less. Additionally, at the back part of the advancing blade, there are negative pressures. According to these pressure distributions, a greater force is generated in the advancing blade, in turn contributing to the generation of torque. On the right in Figure 18 is the pressure distribution when the rotor is parallel to the flow; there are no significant differences in the pressure distributions in the two blades, being this the point with the lowest torque.

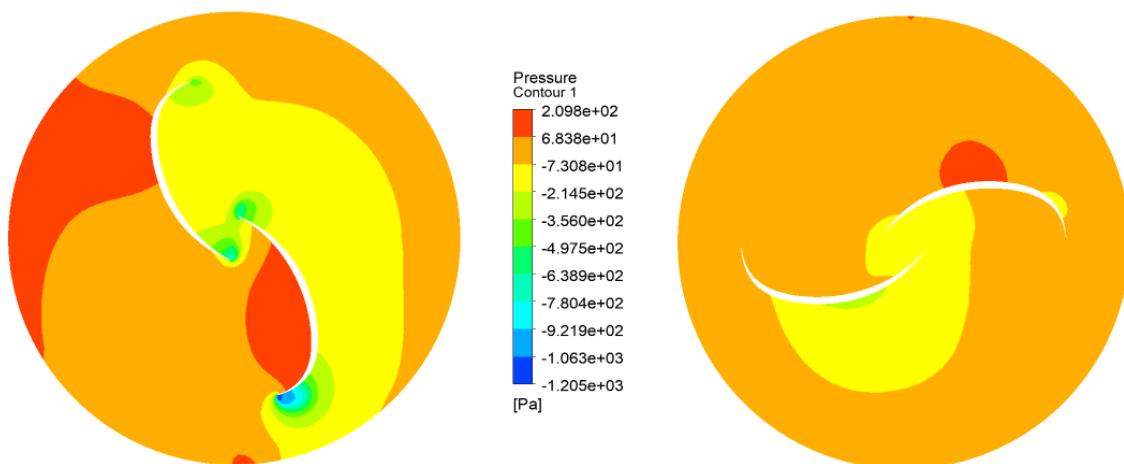


Figure 18 Profile pressure contour at different points of rotation (for a speed of 10 m/s at a TSR of 0.8)

CFD simulations are performed to evaluate the performance of the designed turbine; for this, a rotor with each of the selected profiles and the geometric characteristics of the rotor presented in the previous section, are simulated at different speeds. The performance of the rotors with each of the profiles is compared and also the performance that would be obtained by modifying the geometry of the profile for speeds greater than 3 m / s (see Table 5).

Table 5 – Design rotor performance

Geometry 1	Geometry 2	Variable Geometry
------------	------------	-------------------

V (m/s)	Ω (rad/s)	T (Nm)	C_p	P (W)	T (Nm)	C_p	P (W)	T (Nm)	C_p	P (W)
3	13.333	0.0447	0.1669	0.5962	0.0431	0.1607	0.5741	0.0447	0.1669	0.5962
6	26.667	0.1786	0.1667	4.7637	0.1842	0.1719	4.9110	0.1842	0.1719	4.9110
10	44.444	0.4846	0.1628	21.5374	0.5089	0.1710	22.6190	0.5089	0.1710	22.6190

The variable geometry rotor uses the best performance of Geometry 1 at low speeds, and the best performance of Geometry 2 at higher speeds. Figure 19 shows the power curves for the rotors with Geometries 1 and 2 and the variable geometry rotor. With the latter it is possible to obtain a better rotor throughout the operating regime. The curve shows the power coefficient at different speeds instead of different TSR because the last one is trying to keep constant at 0.8 by means of the generator, as mentioned previously.

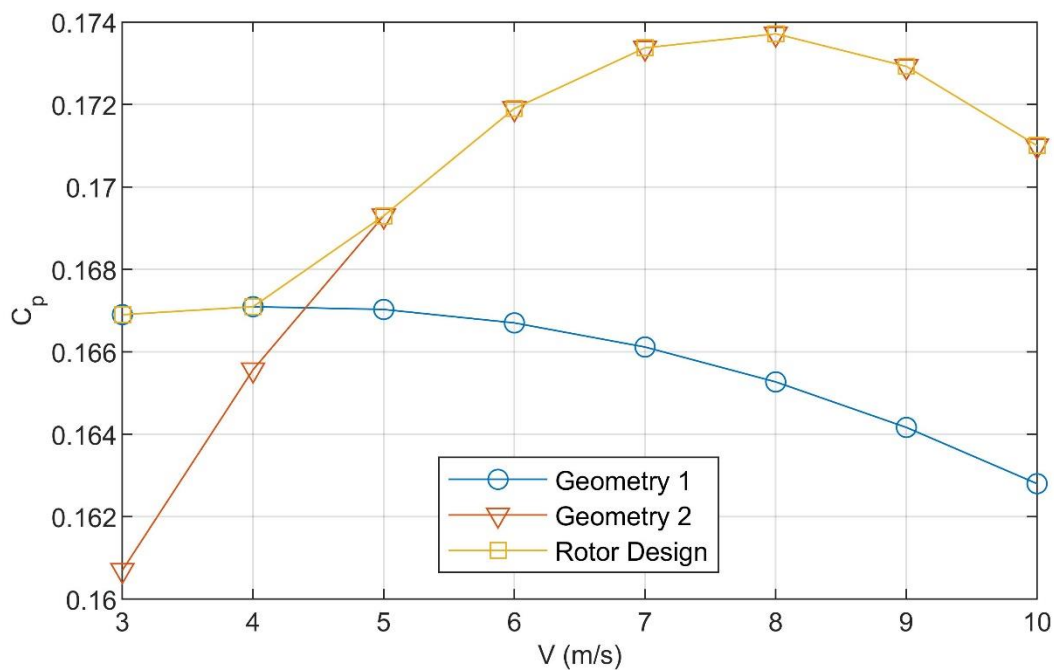


Figure 19 Power curves for the different geometries and the designed rotor

Figure 20 shows the behavior of the flow in its interaction with the rotor. It is evident how this is not uniform, the flow lines are not completely horizontal, but tend to deviate a bit towards the upper and lower ends of the rotor. This is due to the effects that occur at the extremes of the rotor. This phenomenon is not taken into account in two-dimensional simulations, which is why the three-dimensional evaluation of the rotor is important, with this, more reliable results are obtained.

Figure 21 shows the pressure distribution in the rotor. Again it is seen that this distribution is not completely uniform, so the importance of three-dimensional simulations is reiterated. This pressure distribution is obtained when the rotor is completely facing the wind. On the left you can see the distribution from the front, while on the right the distribution from the rear of the rotor is shown. It is observed that the area of highest pressure on the surface of the rotor occurs in the receding

blade, however, this high-pressure area occurs in a specific area of this blade, in the rest of the blade there are quite enough minor pressures and even negative, making the resulting force in this blade less than that generated in the advancing blade. In this last one, the pressure peak is not so high, but there are relatively high pressures in most of its surface, in addition to negative pressure sections in its rear part. The area of greatest pressure in the advancing blade is further away from the rotation axis, contributing even more to the generation of torque.

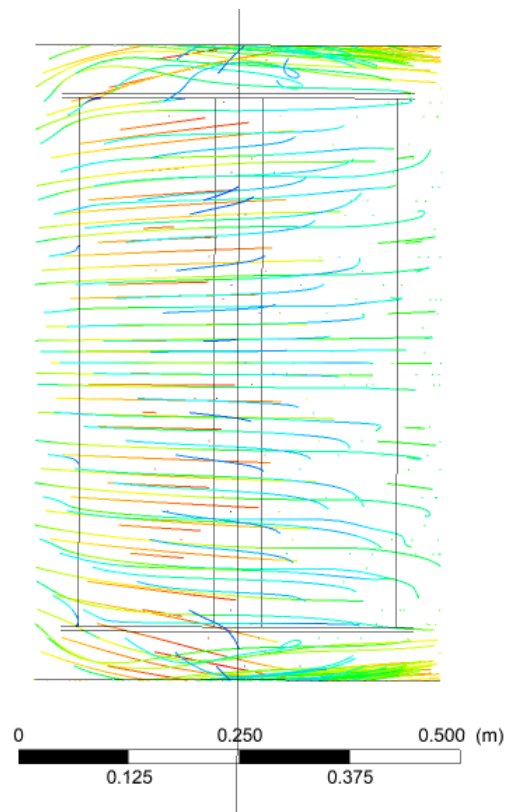


Figure 20 Current lines on the rotor. Own elaboration

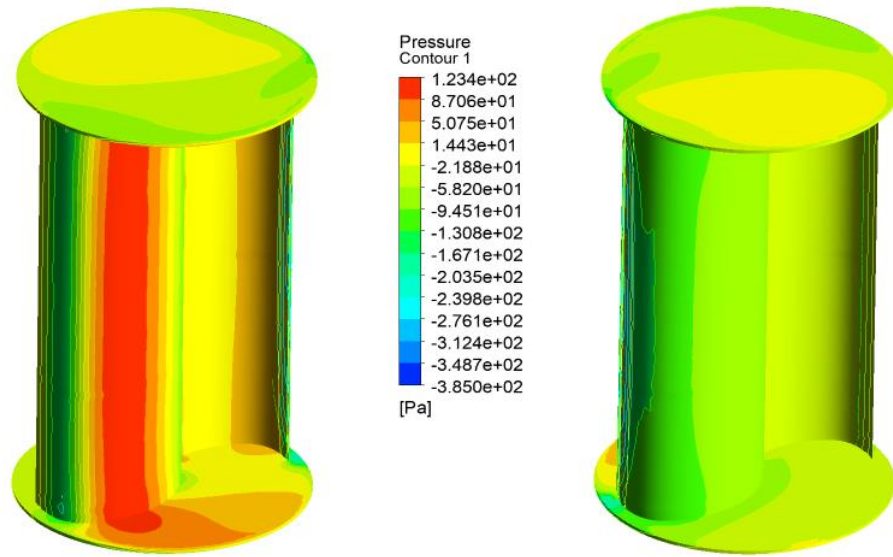


Figure 21 Pressure contour in the rotor when the wind hits the blades head-on. Viewed from the front (left) and viewed from behind (right). Own elaboration

3.2 COMPARISON OF ROTORS BY POWER GENERATION

To compare the variable geometry rotor with the fixed profile rotor in a more intuitive way, the annual energy production is estimated if they operate in the city of Medellín (Colombia). In this area the wind is variable, in addition to having low speeds, around 3m / s, it also has high speeds, more than 6m / s. The well-known Weibull distribution is used to estimate the annual energy production. This distribution models the probability that the wind speed takes certain values [49]. This distribution depends on the area, so certain characteristics of it must be known, represented by the scale parameter S and the shape parameter k .

$$h(V) = \frac{k}{S} \left(\frac{V}{S}\right)^{k-1} e^{-\left(\frac{V}{S}\right)^k}$$

Where h is the probability that the wind will pick up a certain speed. To calculate the annual energy production, the range of speeds is discretized and the possibility that the speed is within a certain subinterval $[V_i, V_{i+1}]$, is calculated, this way for each subinterval representing the average speed in it.

$$h(V_i < V < V_{i+1}) = e^{-\left(\frac{V_i}{S}\right)^k} - e^{-\left(\frac{V_{i+1}}{S}\right)^k}$$

Knowing the power obtained at each evaluated speed, the annual energy production of the rotor can be estimated.

$$Prod\ Annual = \sum \frac{1}{2} [P(V_i) + P(V_{i+1})] h(V_i < V < V_{i+1})$$

The scale and shape parameters for the city of Medellín are found in the IDEAM interactive atlas [69] ($S = 3\text{ m/s}, k = 2.5$).

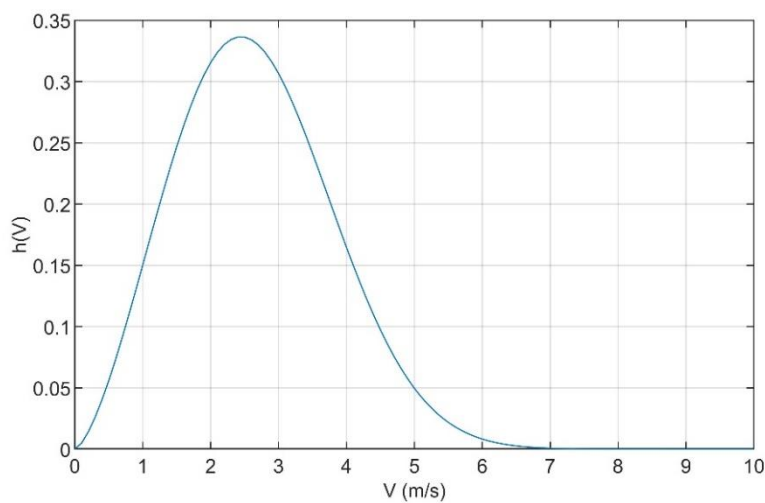


Figure 22 Probability distribution for wind speed in Medellín [77]

It is observed how the speed generally varies between 0 and 7 m / s, with an average around 2.5 m / s.

Table 6 – Annual production of geometry 1 and 2 and the variable rotor

	Annual Production (kWh)
Geometry 1	4.5017
Geometry 2	4.4993
Variable Rotor	4.5441

The obtained design would generate 45 Wh more in the year, and the efficiency is on average 3% better when compared to the best rotor with a fixed profile, that is Geometry 1. This annual saving is not very high. The designed geometry performs better than Geometry 1 at low speeds, while at high speeds the behavior is very similar. At high wind speeds it is when more energy is available in it, so at low speeds, no matter how efficient the rotor is in this regime, it does not contribute much

to the generation of energy. It is more important to design a rotor that is as optimal as possible at high speeds, considering that it is better to take advantage of this speed regime to the maximum; this taking into account the range of speeds in the area, mainly its higher speeds.

4 RESULTS FOR CHANGING THE TURBINE GEOMETRY AND STIFFNESS

4.1 PROPOSED SOLUTIONS

4.1.1 SOLUTION 1

In the following solution, a change in geometry is proposed through automation: the turbine will have a system underneath that will change the geometry of the blades. Its function will depend on the wind speed which will be calculated by means of a sensor. When the sensor detects a change in the speed limit, it waits an assigned time, then stops the turbine and proceeds to change the geometry for one that is better for the wind condition that is present, and thus this new geometry takes advantage of this speed to generate more power than the other geometry.

The system consists on the following: when the sensor detects the change in the speed limit (from low to high speed or from high to low speed), it will wait a while (with a timer) because the speed can remain constant near the limit or it could return to its previous speed. If these previous conditions are not met then the system will proceed to make the geometry change. Magnets would be used together with a friction brake, in order to stop the turbine as soon as possible. The magnets (energized coils) are used to stop the turbine at the exact point where the outlet for the new pair of blades (Figure 23 and 24). In turn, in this position where the turbine stopped, another outlet will be located to extract the geometry that was previously. The blades will be extracted/added by means of two pistons, one for each pair of blades. The first piston would be the one that would extract the geometry to be changed, the piston and the blades would be attach through magnets in order to be extracted. After the piston returns to its initial position, the second piston would come out with the new pair of blades. This will put them in the proper position and then the pistons would lower to their initial position, deactivating the magnets so that the turbine begins to rotate with the new given geometry.

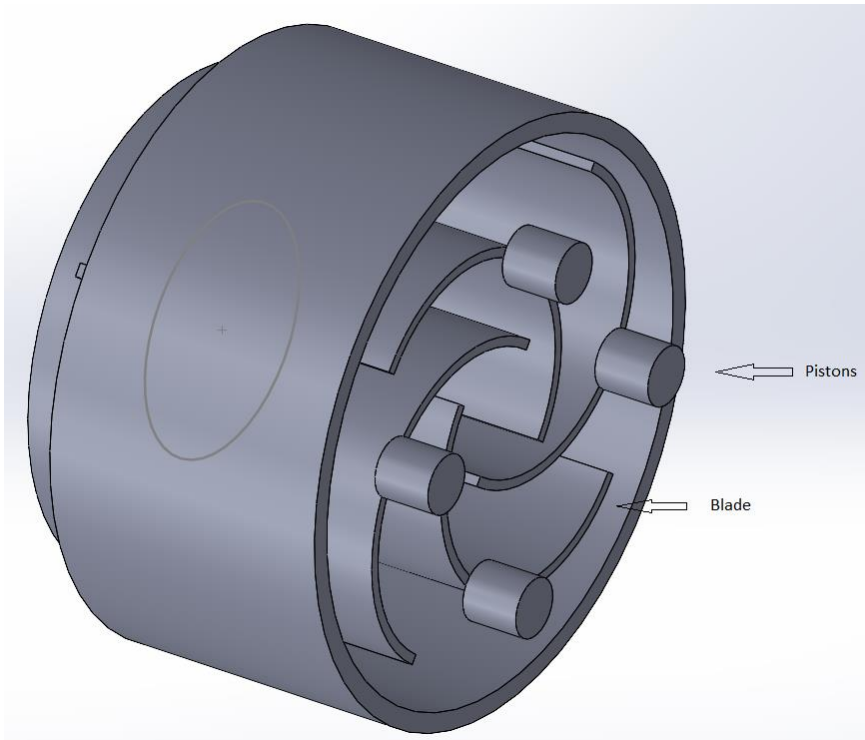


Figure 23 Isometric view of solution 1. Own elaboration

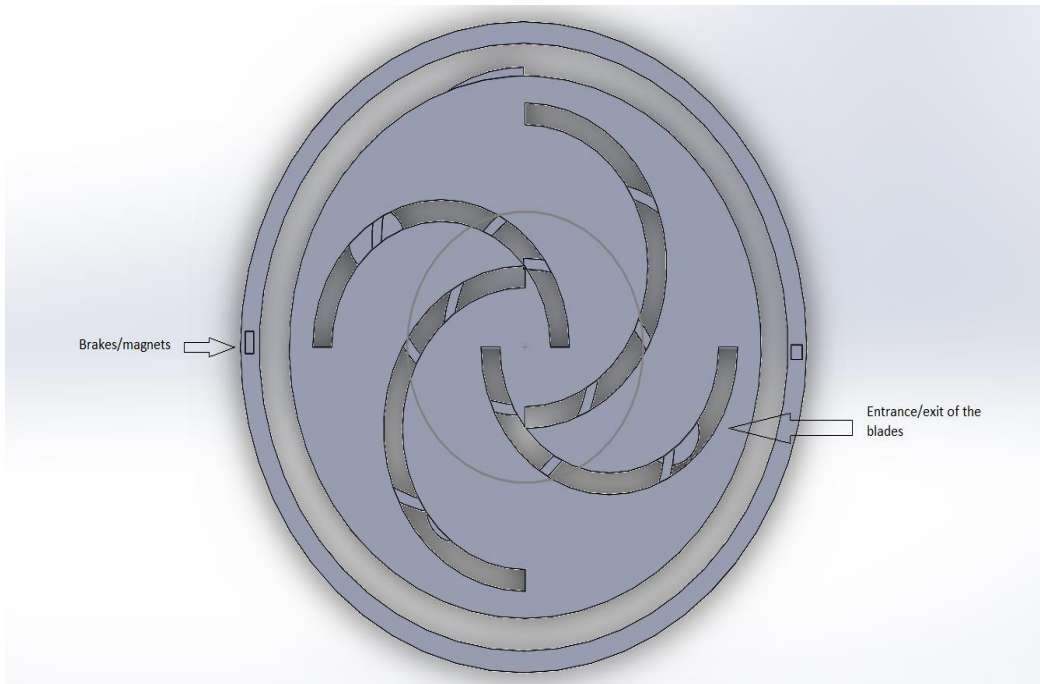


Figure 24 Bottom view of the solution 1. Own elaboration

4.1.2 SOLUTION 2

For the next solution, the following will be presented: a manual blade change. It consists of a "buildable" Savonius turbine like figure 25, which is composed with a pair of blades together with the upper part, forming a single piece. With two different pieces, one for low speeds and the other for high speeds, the geometry change of the Savonius turbine would be done manually.

For this, two pieces with different geometries will be used, through a sensor it will be known if the wind speed is high or low, and with this, a person would proceed to make the manual change of the turbine. For this, the person will proceed to remove part 1 from above, removing the upper part that will be attached with the blades, for this, the person would remove a lock and extract the complete part, and immediately proceed to put part 2 with a different geometry. To insert part 2, it is simply placed in such a way that the blades fit on the disc that has the shape of the geometry of the blades of part 1 and 2. This would be a non-energy consuming way, but it would take a person to make the switch when needed.

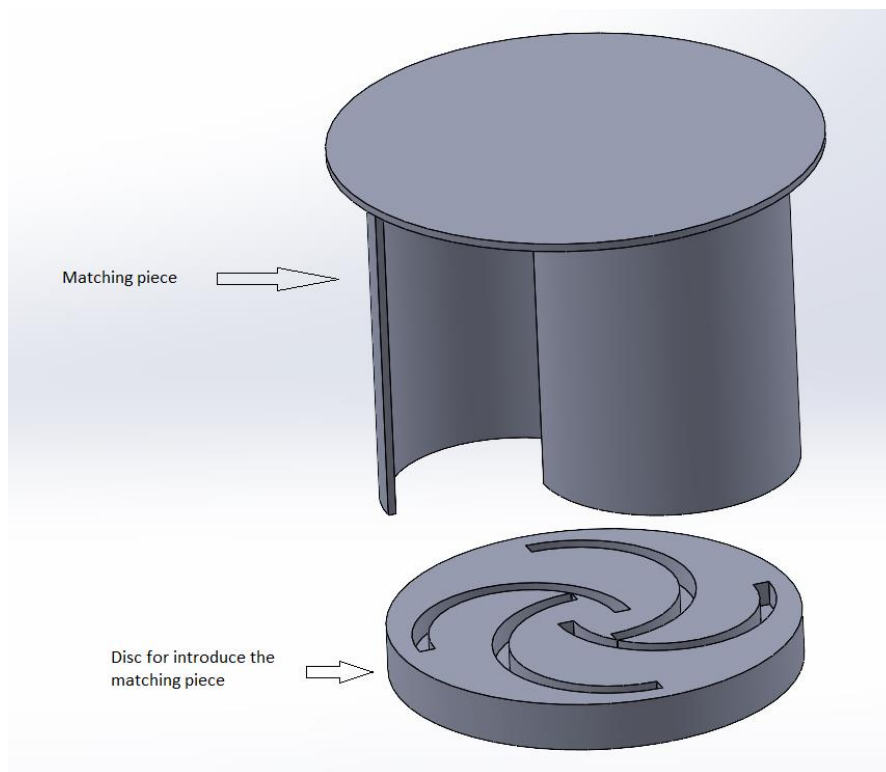


Figure 25 Separated turbine by its two pieces, B (bottom piece) is the base and A (top piece) is the piece to be changed (there will be two A pieces but with different geometries). Own elaboration

4.1.3 SOLUTION 3

In this solution, we will propose the use of different “pieces” to form the blade geometry required for each wind speed. The geometry of the turbine will consist of five pillars per blade, which are columns, which will all be covered by an elastic fabric. Only three of the five pillars will move to find the required geometry for each wind speed.

The turbine would have a total of 8 points with 5 pillars, of which the first and last will remain fixed while the other three will be able to move from one point to the other respectively, as seen in the figure 26. Between these six points (the three that will be connected to each other) there will be a path where the pillar will move until it reaches the point where they will fit to form the new geometry. By means of a sensor, the wind speed will be measured in order to move the pillars to the position that forms the blade, which would be the most optimal for that speed (low or high).

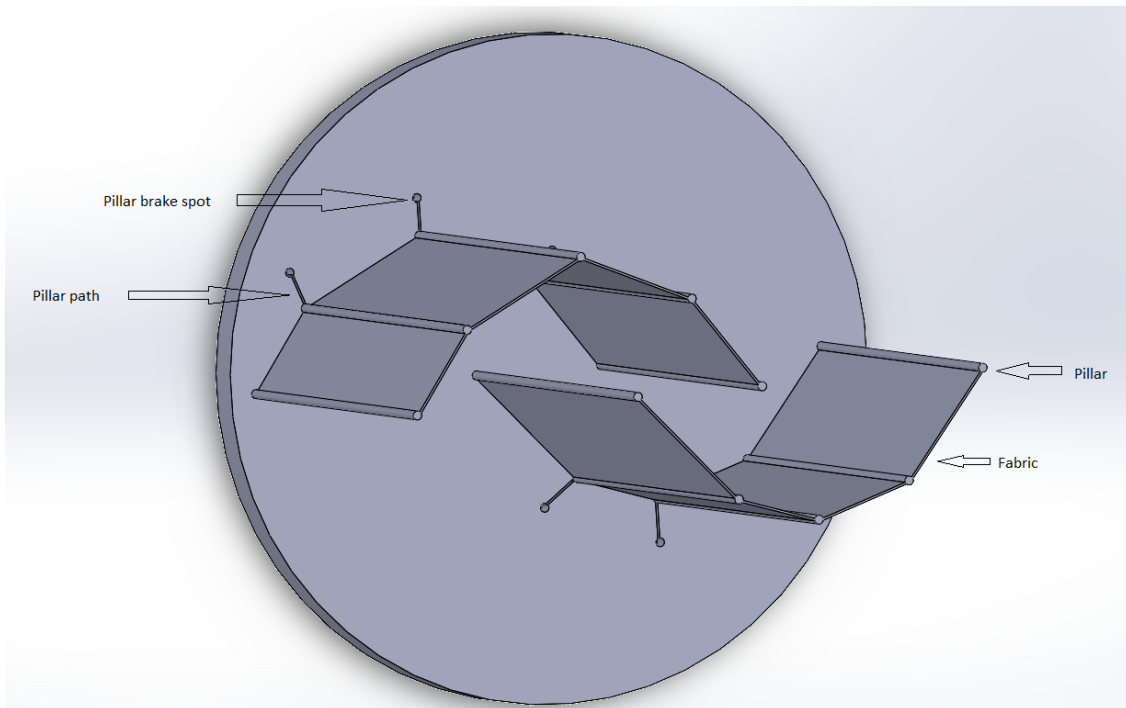


Figure 26 View of the blades with their two shapes that it acquires depending on the wind speed.
Own elaboration

4.1.4 SOLUTION 4

For solution 4, a turbine which the blades will be made with a waterproof and elastic fabric. The pair of blades would be in an initial position being stretched by a system that would be controlled by springs as seen in figure 27

The turbine will be made of two blades that are composed by an elastic and waterproof fabric, that will be connected with a spring at both ends. At the ends of the turbine there is a column connected with a spring that is connected to the fabric. Along with a "path" that is part of the turbine, where it would be the only point where the spring would stretch, this in order to move the column and

generate the respective form of the blade that best fits when reaching high speeds. At the center point of the turbine, where the blades begin, there will be one fix column for each blade, the fabric will be attached here. For the extremes, there will be one column which will move in a path to follow, this column will move in a parallel direction towards the other column of the center. This would be the dynamics for solution 4, without the use of other devices, just fabric and springs.

The operation would be as follows: the initial blade shape will be form because of the springs that would be in their initial shape. This initial shape would be an optimal shape for low wind speeds and for making the turbine able to have a self-start, since the It will be fully stretched, thus having greater rigidity so that the wind can affect its entire area and generate movement. As the wind increases in speed, the fabric will function like a boat sail, which will pull the springs from the column and the center of the blade, until it reaches an end point, forming a new form of blade which is more efficient. for high speeds and at the same time it has a low stiffness so that it can more easily reach the new blade shape, which would give less incision area for the wind and thus avoid damaging the turbine, and at the same time, keep the efficiency constant.

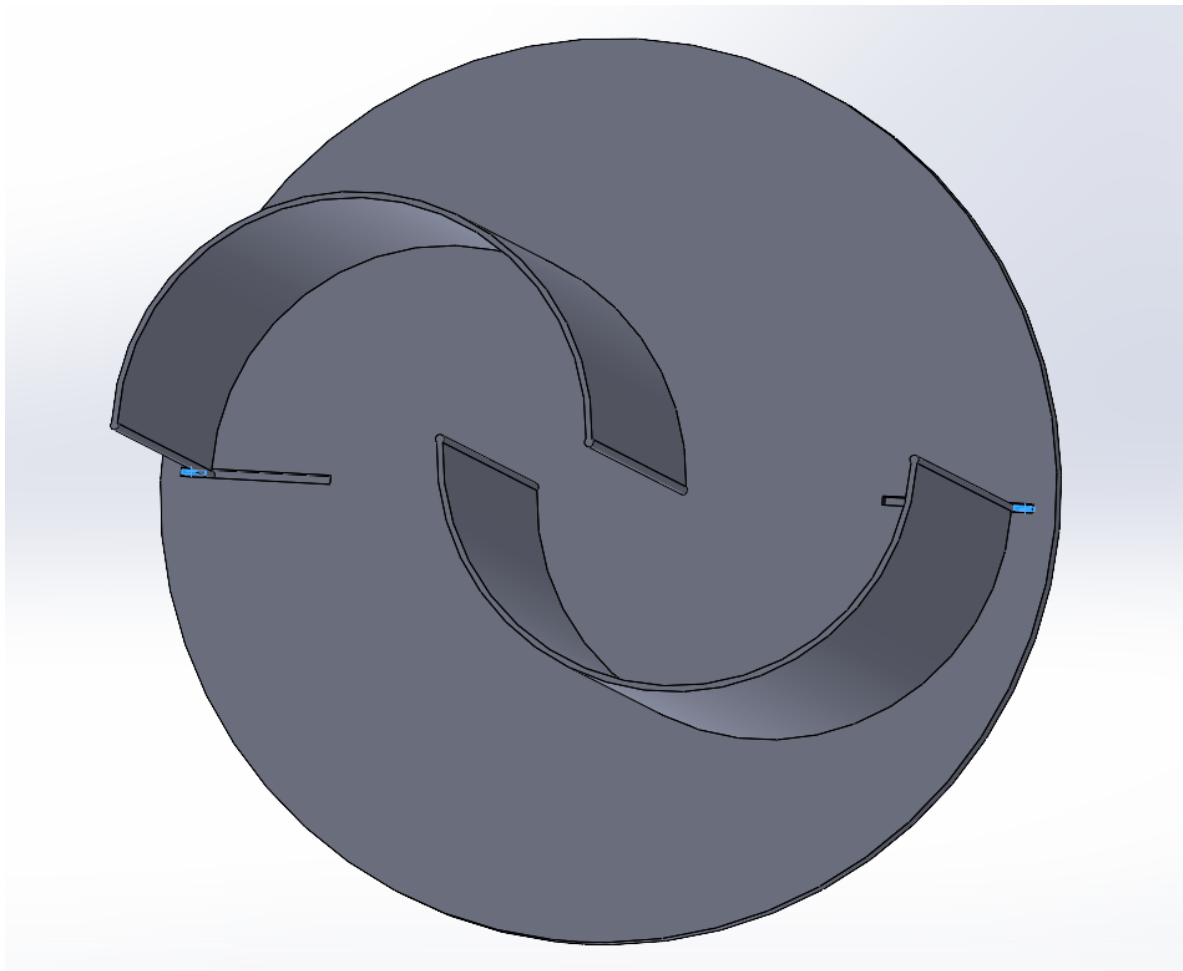


Figure 27. View of blades (made with fabric) next to the springs (blue)

4.2 NUMERICAL ANALYSIS OF THE PROPOSED SOLUTIONS

In order to compare how much impact, the mechanism of the geometry change has on the performance, additional simulations are performed to obtain the rotor efficiency curve in each case. It is evident that solutions 1 and 2 are going to have a much better performance than solution 3, since the geometry that this last one can take may not be faithful enough to the design, changing the behavior of the flow around the blades, and with this, their performance. The performance of the different solutions is further compared to a conventional Savonius rotor for reference. This is the one presented in the validation section of the 3D model for the evaluation of the obtained design [75].

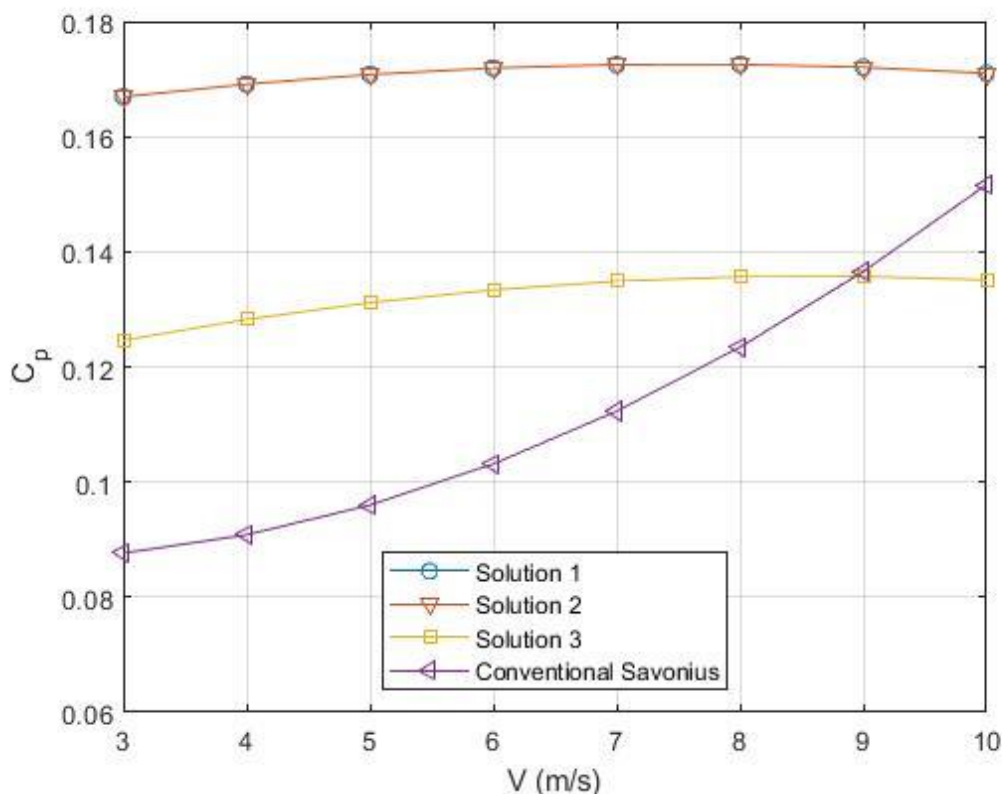


Figure 28 - Comparison of the performance of the different proposed solutions.

Despite the fact that solution 3 has a much lower performance than the other two alternatives, it still presents better performance than a conventional Savonius at low speeds (in this case, below 9 m / s). In the performance graph of the conventional rotor you can see a considerable increase as the operating speed increases. At speeds greater than 10 m / s it may be even better than the rotor designed in this work; however, the purpose of the rotor being designed is its versatility of operation at low speeds, and according to the graph, this is satisfactorily accomplished. Since the rotor operation is fixed at TSR = 0.8, a graph of power coefficient versus TSR is not presented, since the latter is intended to be kept fixed. That is why the utility of a power versus speed coefficient graph shows us, in a more convenient way, the performance of the designed rotor and how it changes if one or the other of the proposed solutions is applied.

4.3 DECISION MATRIX

To select the best solution, we proceed to evaluate five important aspects of each given solution: Geometry shape fidelity, estimated cost, independence of operation, solution complexity, and solution reliability. A score of 1 to 5 will be given to each aspect for each solution, calculate the average and thus choose the best system of the 3 proposed solutions.

- **Geometry shape fidelity:** The ability of the solution to mimic the geometry exactly is discussed. For solutions 1 and 2 we can see that they have a very high fidelity, since the blades faithfully imitate the geometry of the blades of the simulations for both high and low wind speeds, for this they will receive the highest score. Solution 3, being composed of a low number of pillars that move to generate the blade change, would not faithfully imitate the geometry for both large and small wind speeds, for this reason, this solution would receive a low score. For solution 4, the fidelity is not entirely exact, for low wind speeds (initial shape) it would have almost an exact shape while for high wind speeds it would not have a shape fidelity, since for this it represents a highly variable behavior due to how easily the material would change shape at that point. This is why solution 4 would receive a low rating.
- **Estimated cost:** about the approximate total cost of each solution, a good solution would also present an acceptable cost. Since these solutions, in general, also seeks to generate savings, so a good solution should also generate an acceptable cost to be accepted by a company. The higher the estimated cost, the lower the score for the proposed solution. For solution 1, we see that it is highly automated: four pistons plus the generation of 4 blades (with 3D printing), sensors and the installation of the system, the maintenance of the system is also taken into account. With these values, solution 1 would have the maximum cost value for which it would be given the lowest score of the 3 solutions. The third solution, although it is also automated, will have a lower cost than the first because it will require fewer objects. For the second solution, the cost depends on the manufacture of the blades and the payment to the person who would be in charge of changing the turbine part, also it would not have maintenance costs, and therefore its estimated cost would be lower than the other solutions. Solution 4 would have the lowest cost of all, since it does not depend on any electronic device for its operation, it would only be spent on the printing of the turbine plus the fabric, the springs and their installation. For this it would receive a high score
- **Independence of operation:** It is linked to how automatic the solution is. For solution 1 and 3 we can see that they are very automatic, especially solution 1, which depends on more components that must communicate with each other to function correctly, therefore it will have a higher score than the third solution. Solution 2 is not fully automatic, it would only depend on a person to make the change and a sensor to know the wind speed, and therefore, it would receive the lowest score of the three solutions. For solution 4, it would have the highest score by having absolute independence, since it does not depend on any electronic device for its correct operation.
- **Complexity of the solution:** It is linked to the number of elements that each proposed solution has, the more elements it has, the more complex it will be and its final score

would be lower. Solution 1 is the one with the most elements and each one must communicate with each other to perform its function well, so this solution would have the lowest score. The third solution depends on fewer elements than the first, so it would have a higher score than the first. The second solution only has 2 pieces, although it depends on a person and a sensor that tells the wind speed, therefore it would have the highest score of the three. Solution 4 would not have a high complexity, since it does not have many elements and none of them are electronic so that means that none of the elements communicate with each other, since it is an autonomous solution. So, solution 4 would receive a high score

- Reliability of the solution:** We will discuss how confident we are that the solution will work. The complexity of the system and the possibilities that there may be a failure will be analyzed. Due to the high degree of automation, we know that the first solution will have a high reliability since the form and methods to be used have been investigated, also because human intervention is not necessary (only for maintenance), so it will not be subjected to human error. Solution 3 would have a medium reliability because it is an experimental method, that is, not much has been experimented on, and therefore it would require more research. Solution 2 would have a probability of failure because the intervention of the human being is present in the equation, it should be taken into account if the person who makes the change does it correctly and constantly, this probability of human error affects the solution 2 score. Solution 4 is not fully studied and applied, it also depends on a fabric and springs so there is not a way to extract data to monitor and control its behavior, so its reliability would be low

Deeply analyzing these 5 aspects, each solution is given its respective score, then the total average is obtained in order to choose the proposed solution, which would be the one with the highest average score. Below, the table 6 with their respective scores.

Table 7 –Decision matrix for each proposed solution

	Solution 1	Solution 2	Solution 3	Solution 4
Geometry shape fidelity	5	5	2	1
Estimated cost	1	3	2	4
Independence of operation	5	2	4	5
Complexity of the solution	1	4	3	4
Reliability of the solution	5	2	3	1
Average score	3.4	3.2	2.8	3.0

With the following decision matrix, we can see that the first solution would be the most reliable, it makes sense since the world is constantly changing due to automation, so a proposal with this topic would be the most reliable to obtain better results and with less error. It has its drawbacks, but further research could improve it further.

With solution 4, its low cost and independence makes it another good solution to be implemented, but also need to be study more for possible solution to control better the blades

4.4 SYSTEM OPERATION FOR THE CHANGE OF GEOMETRY AND STIFFNESS

Each solution will be made up of several components that will interact with each other to generate a correct operation. For solution 2 it would be the simplest of all, since it will only need 2 pieces with a different blade geometry, a wind speed sensor to know when to make the manually change and the installation of the system along with other materials plus unexpected events.

Solution 1 and 3 have almost the same materials, although their operation and installation will be different. For the materials, they will be composed of pneumatic actuators to make the blade change, a wind speed sensor to know when to make the change, proximity sensors to know at what specific point the turbine can make the change, and a microcontroller to connect all these components together so that they can interact with each other when making the blade change.

The differences between solution 1 and 3 would be the blades, while solution 1 will be composed of blades made in 3D printing, solution 3 will be composed of an elastic fabric and several columns to generate the required blade shape. Its installation will be different, as its behavior when changing the blade geometry and also the algorithm created by the microcontroller will also be different.

Next, the explanation of the operation of each solution together with the elements by which it will be made up

4.4.1 SYSTEM OPERATION FOR SOLUTION 1 AND 3

The operation of the system would be as follows (applies for solutions 1 and 3): the turbine will be rotating initially with the blade geometry that is the most optimal for the wind speed that is being presented. In turn, the data from the wind speed sensor will be constantly collected and analyzed. When this data meets the condition of passing a limit (to consider that it is going from low to high wind speed or vice versa) a timer will be activated (generated in the algorithm with the Arduino microcontroller). As long as this condition of having passed the limit is fulfilled together with the termination of the timer, then the blade change will be carried out. If the condition is not met in the estimated time, the blade change will not be carried out and the turbine will continue to rotate as it was initially. For the limit, it will be stated that the wind speed must be greater than 5 m / s to be considered high wind speed, while if it is less than 5 m / s it will be considered low wind speed. The timer will be 50 seconds, which indicates that to make the blade change, the information from the wind speed sensor must have changed condition and remain in that condition for at least 50 seconds.

For the geometry change, the turbine will be braked, this will be done when the speed change condition is met. For this, a brake will be activated to slow the turbine to a specific point. For this specific point, 2 proximity sensors will be used and must be turned on at the same time for a short time to indicate that the turbine has been completely stopped. When this condition is met for the two proximity sensors, it will mean that the turbine is in the right position to make the change of the blades.

While the two proximity sensors are activated, the system will proceed to send a command to the actuators to go out to pick up the blades, when these actuators are fully retracted, the other actuators will proceed to exit together with the new pair to be placed. Once the new geometry is installed, the actuators will return to their initial position, when they are fully retracted, the brake will be removed so that the turbine will start to rotate again together with the new pair of blade installed. This process will be repeated when a speed change is detected that remains above or below the given limit for more than 50 seconds. The blades will enter and exit through a folding gate that will only be opened when they have contact with the actuator. This would be the behavior of the blade change of solution 1

For solution 3, the behavior would be different at the moment of the change: the pair of blades will not be changed, but the geometry of the blade already present will be changed. For this process, the following will be carried out: the actuators used will be placed vertically, parallel to the ground and the rotor, there would be two actuators to make the change in geometry and another pair to return the blades to their initial position (which would be for low wind speeds). The three central columns of each blade will be connected to each other at the bottom by a vertical column, this in order to use only one actuator per column. When the condition of the proximity sensors next to the timer is fulfilled, the actuators will push the column and thus move the 3 central columns of the blade at the same time, until reaching a specific point where a lock will close to leave the columns in the new position. To return to the initial position, the other pair of actuators would push the columns back to their initial position.

4.4.2 SYSTEM OPERATION FOR SOLUTION 2

The wind speed data will be collected by a wind speed sensor, when the speed is higher or lower than an indicated limit, a timer will be activated, if the timer ends and the wind speed continues above or below the limit, the blade change will be carried out manually. This manual change will be carried out by one person, for the moment the change will be made in this way, although in the future it is expected to find an easier, more precise, faster and cheaper way to make the change.

4.4.3 SYSTEM OPERATION FOR SOLUTION 4

For the operation of solution 4 we have the following: having absolute independence, then it would not be needed for any electronic devices such as actuators, sensors and a microcontroller. The turbine is printed with a 3D printer, with the specifications of the solution: it must have a not so deep line at the bottom where the springs would be installed next to the columns. These lines would be the paths that the column would travel in order to drag the fabric and give the new blade form. In these roads the columns would be dragged because of the force in which the fabric drags them, this would be due to the force of the wind, since, if it is at high speeds, when impacting on the blade, it would drag it up until its final point, where at that point the new form of the blade would be formed, been this shape the most suitable for high wind speeds. When the wind speed decreases, the force that is incident on the blade will decrease and the springs will take care of returning the

columns to the initial point, as long as the wind speed is low enough to allow the springs to return the columns to its starting point.

Initially, the blade would have a suitable shape for low speeds, which is due to the fabric fully stretched by the springs, thus giving more area for the wind to impact on it and move the turbine. When the columns reach the second point and form the new blade form, this new shape would have less area, so it would be easier to bend it, which would cause the turbine to take advantage of these speeds, avoiding to damage the turbine by rotating at very high speeds, giving thus greater energy and durability of the turbine.

In summary: when the wind has a high speed, the force on the fabric will increase, this will deform the spring and the fabric, making the blades more concave, and for this reason the stiffness of the materials and the structure will change. When the wind speed is less than the force exerted by the spring on the turbine at that point, neither the spring nor the fabric will deform considerably.

4.5 SOLUTIONS COST

For each proposed solution, the approximate quote to be made will be analyzed.

4.5.1 BLADES MANUFACTURING

First, the creation of the blades is analyzed, in which, in order to obtain its shapes with greater accuracy, the design would be made by means of a Software and then printed by a 3D printer. This process is called additive manufacturing. For solution 1 and 2, more time would be required because the 2 different pairs of blades would have to be manufactured, giving an approximate of 32 hours for the additive manufacturing for solution 1. For solution 2 it would be a little more time because there needs to be made 2 full removable turbines with their pair of blades. In Colombia, several of these fabrications have an approximate cost of 30,000 Colombian pesos per hour (7 euros / hour) thus giving us an approximate total of 960,000 Colombian pesos (224 euros) and approximately 250 euros for solution 2. For solution 3 the cost It would be less because a "skeleton" should be made where the flexible fabric needs to be, so the price for the third solution would have an approximate of 120 euros

For solution 4, the highest cost would be the printing of the turbine with the required specifications to be able to install the columns and the fabric, among these impressions the columns would also come.

4.5.2 ACTUATORS

For the actuators, linear actuators will be used, for solution 1, four linear actuators will be needed, of which one pair would extract the blades while the other pair would put the new blades. These linear actuators must have a length greater than the height of the blades. If the turbine designs have

a height of 0.5 meters then the linear actuators should have a height of approximately 0.6 m. For a total of 4 actuators with these conditions, they would have an approximate cost of 250 per actuator for solution 1. For solution 3 the actuators will be shorter since they will be installed parallel to the ground. So, as the radius of the turbine is approximately 300mm, then 4 pistons of length of 150mm would be the indicated for solution 3 and it has an approximate cost of 150 euros per unit. The actuators are the main components for solution 1 and 3. The best actuator is a pneumatic type, since they are not only the cheapest, also they are the ones with the best precision.



Figure 29 Pneumatic cylinder actuator. Image taken from the Festo catalog

4.5.3 SENSORS

For the sensors, we will first analyze the traditional sensors for wind speed, that can measure accurately and in a reliably way, the wind speed in all kinds of environmental conditions. These sensors also have a good performance against extreme weather conditions and can also measure low speeds. These sensors are effective for the areas where the proposed wind turbines would be applied. They have an approximate cost of 150 euros. This type of sensor is essential for every proposed solution.



Figure 30 PCE-FST-200-201 Wind Sensor. Image taken from the pce-instruments catalog

The other sensors would be inductive proximity sensors, which would be used in solution 1 to activate the pistons once these sensors are activated for a time, indicating that the turbine has stopped in the proper position to extract the pair of blades, and in then, install the new pair. These sensors have a low cost of approximately 10 euros per unit, so a pair would have a value of approximately 20 euros.



Figure 31 Normally Open Inductive Proximity Sensor. Image taken from the Amazon catalog

4.5.4 MICROCONTROLLER

For the sensors and actuators to communicate with each other so that solutions 1 and 3 work in a synchronized manner, they must have a microcontroller. By means of an algorithm use to give commands and connections of each device through wires, the microcontroller can generate the correct operation of each component of the turbine and thus generate the blade change without error. The microcontroller used will be the traditional Arduino, which has a value of 25 euros.



Figure 32 Arduino microcontroller. Image taken from the Amazon catalog

4.5.5 OTHER MATERIALS

For the fabric in solution 3, polyester with high porosity (percentage of empty spaces in a formation that can contain fluids) is used since this would prevent the passage of air through the fabric so the turbine could rotate, it is also a flexible material, which is essential for generate the change in the geometry of solution 3. The cost of this type of polyester fabric, with the necessary dimensions to cover the entire blade of the proposed solution, would have an approximate value of 20 euros.



Figure 33 Flexible waterproof polyester fabric. Image taken from the Amazon catalog

For the springs, a pair will be chosen that contains the necessary measurements as well as its elasticity constant to be able to generate the blade changes depending on the force that the wind

imposes on the blade. A variable area and stiffness will be obtained, since as these two factors change, the force that affects the blade will also change, but as these factors increase, it means that the wind speed is also increased, which means, they are directly proportional. Therefore some (traditional) linear sensors will be used. For this type of spring, several springs between 2 and 3 centimeters will be analyzed, since several tests must be carried out, therefore, a number of sensors with low length and constant elasticity will be used. A box with several of these springs has an approximate cost of 10 euros

For other materials (cables, screws, etc.) an approximate percentage for each proposed solution will be used. This percentage would be 10%, to have a safe value to obtain all the secondary and necessary materials of each solution. For the unexpected it would be 15%, in which it is to anticipate any emergency or problem that may arise, also for elements that were not considered and any additional tooling.

Additionally, for solution 1 neodymium magnets will be used, which are known for their magnetic strength and low cost. These will be used at the end of the pneumatic actuator to use the force of the magnet to pick up and carry the blades. These magnets have a cost of 5 euros per unit, which, having 4 pistons, will need 4 magnets, giving a total cost of 20 euros.

4.6 COST SUMMARY

With these data we proceed to make the approximate total cost for each proposed solution

From the following table we can analyze as discussed previously in the decision matrix, solution 1 would be the most expensive, although the most reliable. It can also be seen that solution 2 is the least expensive as it does not have devices that communicate with each other, since it would depend mainly on one person and is not automated. Solution 3, despite being automated as solution 1, its costs are not as high, mainly due to the design of the blades, since instead of using a complete 3D printing, a polyester fabric will be used. The higher cost is due to the pneumatic actuators, since these are the main component to use to make the change of geometry, and with more of these components, then more cost for their maintenance and repairs. Future solutions will be studied, one could be the use of only two actuators and further automate the system to perform the blade geometry change with only two actuators. One solution would be to have the actuators in a rotary system so that the same actuators can be used to make all the geometry changes. This would apply for solution 3, for solution 1 it would be necessary to apply another system that contains the blades that are saved and thus the actuators are free to carry out the change.

Table 8 - Table Values of each element together with the total for each solution

	Materials	Unit Price	Quantity	Total	Total of the Solution
Solution 1	Blades	224	1	224	1798,75
	Pneumatic actuators	250	4	1000	
	Wind velocity sensors	150	1	150	
	Proximity sensors	10	2	20	
	Arduino	25	1	25	

	Magnet (Neodymium)	5	4	20	
	Other materials	15% of total	1	143,9	
	Unforeseen expenses	10% of total	1	215,85	
Solution 2	Blades	300	1	300	562,5
	Wind velocity sensor	150	1	150	
	Other materials	15% of total	1	67,5	
	Unforeseen expenses	10% of total	1	45	
Solution 3	Column for the blades	120	1	120	1168,75
	Pneumatic actuators	150	4	600	
	Wind velocity sensors	150	1	150	
	Proximity sensors	10	2	20	
	Arduino	25	1	25	
	Polyester	20	1	20	
	Other materials	15% of total	1	140,25	
	Unforeseen expenses	10% of total	1	93,5	
Solution 4	Column for the Blades	250	1	250	350
	Polyester	20	1	20	
	Springs	10	1	10	
	Other materials	15% of total	1	42	
	Unforeseen expenses	10% of total	1	28	

Errore. L'origine riferimento non è stata trovata.

As seen in the table the first solution is the most expensive because is fully automated, while solution 2 presents a low cost because only a sensor is used, the rest of is manually operated. Solution 4 is the cheapest of all because it does not use electronic devices, it has absolute independence, also the elements it uses are low cost, although it still needs more research to select the best materials.

4.7 FUTURE WORK AND DISCUSSIONS

In this field it will be discussed about the topics that would be done in the future for this paper, in order to obtain new results and new conclusions.

It will go into further details for to the solution of the variable stiffness, since there are very few researches of it, which would require more investigations to observe the results that would be presented and thus improve the knowledge regarding the subject.

A more in-depth investigation would be made in the materials and components that will be used in the solutions, to obtain a more precise values of each solution and to have selected the companies that will be in charge of supplying these products and also those for maintenance of them.

The application of variable stiffness and geometry to other types of vertical wind turbines, such as the Daerrius, would also be investigated. A focus would be on its design, geometry, equations and simulations in order to find the best geometries for different wind speeds. Then it will proceed to investigate the different solutions to achieve the variability of the geometry and stiffness.

After the results, the most important thing is to discuss more in detail each proposed solutions. The change in geometry and stiffness are two factors that are related to each other when we talk about wind turbines. A change in stiffness will also lead to a change in the shape of the material and vice versa. To change both, several elements and investigations are required that can meet the most important requirements of wind turbines: energy production, efficiency and duration.

For energy production, which is considered the most important factor, the proposed solutions present the following: that to make the respective blade change, energy must be used to make this change, for which a percentage of the energy produced by the turbine must be used. To have a solution without errors, an automated system is required and in which all its elements can communicate with each other for the generation of the change quickly and accurately. This, in turn, requires a good constant use of energy, which must be of very low value compared to the energy produced by the turbine to have a good percentage of produce energy. For this, studies will be required to use devices that use the least amount of energy possible, also reducing the number of devices would help to save energy. Another solution can be to use devices that use another type of energy, such as solar energy. This would be a great field to work in the future to improve the solutions, since what is search is to produce as much energy as possible.

Another important factor that affects energy production is the loss that is generated when the turbine stops at the time for making the blade change and also the time that it takes for the turbine to return to its maximum speed again. For both automated and manual blade changes, it will be required to stop the turbine in order to generate the change and then wait from its self-start until it reaches to its maximum speed. This time interval in which the turbine stops for a time and arrives at its maximum speed generates energy losses, which could be a problem if we find multiple changes of the wind speed in a short time interval. This could generate losses and low energy production, for which several investigations should be carried out, including a more complex algorithm that can generate the least possible amount of geometry changes in a day, analyzing the weather future conditions to predict the number of changes and in what time to do them.

Another solution, but more complex, would be to study the way to be able to generate the change without having to stop the turbine, as is proposed in solution 4, although this type of solution requires deep research, because in turn this solution would generate another drawback: in order to not stop the turbine, the system should have all the elements installed in it, which must communicate and be charged without cables. The problem with this would be that by installing these elements in the turbine, more weight would be added to it, which would lower its maximum rotation speed as well as make it difficult to generate an self-start. It should be studied which elements would be the most suitable and which can produce the blade change with precision and low consumption. Consideration should also be given to how to install these devices (which should be low in weight and mass) and how to keep them charged.

For solution 4, the difficulties are found in the type of material that must be used, both for the elastic fabric and for the springs. Also, the measures that the blades should have and how much their

stiffness must change to generate the greatest amount of energy with each turn needs a deep search. Mainly, in order to obtain these values, a 3D study and simulation are required, since the variable stiffness generates a change in the shape of the blade with greater variation, powerful software must be used in which the most exact behavior of the system can be analyzed. This software requires a lot of power and time to be able to simulate several models in various environments, which can be studied and thus obtain the most approximate data possible of the best solution. With these results, the selection of several materials is carried out to physically generate the solution with the most similarity to the simulated one.

In addition to these problems that must be analyzed in the future to obtain the best version of a Savonius turbine with stiffness / variable geometry. The following proposed solutions can be used as a basis for future research and thus discover other methods to generate the change of stiffness and geometry, taking into account all these factors that are discussed in this chapter. New ideas or new ways to improve the solutions that are already proposed would be the main objective of future works. Other solutions could be given for another type of vertical wind turbine, although a new study of geometries and dimensions is required, it would be a good start to present new proposals and analysis of variable geometry and variable stiffness applied to other types of wind turbines.

5. CONCLUSIONS

A variable geometry Savonius rotor design is proposed, which its variation allows better use of the available energy in the wind at different operating speeds.

In the analysis prior to the final design, it is found that in general, the concavity of the rotor profile has a quite important impact on the performance.

Other geometric parameters such as the location of the point of maximum curvature have some impact, but not very significant, and the range in which it can be varied without seriously compromising the rotor performance is quite wide. The flexibility of this parameter can be used in favor of other rotor factors such as ease of manufacture, simplicity of maintenance, or structural requirements.

The two geometries obtained are quite similar, despite the fact that the increase in the power coefficient is evident. Taking this into account, and what was mentioned above, it can be said that the geometry of the profile has quite an impact on its performance; Small geometric changes can generate considerable changes in performance. Although the increase in the power coefficient is evident, when evaluating the increase in annual energy production, this increase is not so considerable.

It is important to aim to improve efficiency mainly in high speed regimes, where there is more energy available to convert. It may be beneficial to sacrifice rotor efficiency at low speeds if it means an improvement in efficiency at high speeds; this obviously taking into account the range of wind speeds in the area to be operated.

It is also important to mention that this variable geometry rotor would be viable in areas where the wind has a wide range of speeds and these are unpredictable, since its main objective is to adapt to unpredictable changes in speed.

To generate the change in geometry, with the advancement of technology and automation, the best solution (solution 1) will require a fully automated system. Which can make, without human error, the change of geometry and thus make the most of each change in wind speed.

Watching the comparison between the performance of the Solution 1, 2 and 3 it can be concluded that the shape of the blade has a significant impact for the power coefficient. This shows that solution 1 and 2 have the best efficiency because of their semi-ellipse blades form while solution 3 has a lower efficiency because of its pentagon-like form, showing the importance of the geometry of the blades.

Analyzing the second solution, it is shown that a manual solution would also have a positive impact. Despite having human intervention, which could generate failures or not taking all the advantage of the turbine. Manual solutions would have a low cost and a low level of complexity, which could be useful on other researches.

For the fourth solution, is conclude that low cost is also one of the best solutions to implement in this type of wind turbine. It also shows the great importance of systems that are independent,

because it saves money and time for not been monitoring the system all the time, giving more savings. Also, the possibility for further studies to improve its behavior are taken into account, because this solution is still in research.

In conclusion, a wind turbine with variable geometry and stiffness is one of the best options to be able to extract the energy from the wind in the best way possible. As explain, the fact of having different geometries that are optimal for a range of wind speed, would make the turbine adapt to the behavior of the wind in the environment in which it is located, thus being able to offer solutions for renewable energies for all kinds of environments.

6. BIBLIOGRAPHY

- [1] Y. Luo, S. Shao, F. Qin, C. Tian, and H. Yang, "Investigation on feasibility of ionic liquids used in solar liquid desiccant air conditioning system," *Sol. Energy*, vol. 86, no. 9, pp. 2718–2724, 2012.
- [2] V. Masson-Delmotte *et al.*, "Global Warming of 1.5°C an IPCC special report on the impacts of global warming of 1.5 °C above pre-industrial levels and related global greenhouse gas emission pathways, in the context of strengthening the global response to the threat of climate change," 2018. [Online]. Available: <https://www.ipcc.ch/sr15/download/>.
- [3] C. M. Niebuhr, M. van Dijk, V. S. Neary, and J. N. Bhagwan, "A review of hydrokinetic turbines and enhancement techniques for canal installations: Technology, applicability and potential," *Renewable and Sustainable Energy Reviews*, vol. 113. Elsevier Ltd, p. 109240, Oct. 01, 2019, doi: 10.1016/j.rser.2019.06.047.
- [4] W. Q. Wang, R. Yin, and Y. Yan, "Design and prediction hydrodynamic performance of horizontal axis micro-hydrokinetic river turbine," *Renew. Energy*, vol. 133, pp. 91–102, Apr. 2019, doi: 10.1016/j.renene.2018.09.106.
- [5] K. M. Almohammadi, D. B. Ingham, L. Ma, and M. Pourkashan, "Computational fluid dynamics (CFD) mesh independency techniques for a straight blade vertical axis wind turbine," *Energy*, vol. 58, pp. 483–493, Sep. 2013, doi: 10.1016/j.energy.2013.06.012.
- [6] J. Lata-García, F. Jurado, L. M. Fernández-Ramírez, and H. Sánchez-Sainz, "Optimal hydrokinetic turbine location and techno-economic analysis of a hybrid system based on photovoltaic/hydrokinetic/hydrogen/battery," *Energy*, vol. 159, pp. 611–620, Sep. 2018, doi: 10.1016/j.energy.2018.06.183.
- [7] T. Micha Premkumar, S. Sivamani, E. Kirthees, V. Hariram, and T. Mohan, "Data set on the experimental investigations of a helical Savonius style VAWT with and without end plates," *Data Br.*, vol. 19, pp. 1925–1932, Aug. 2018, doi: 10.1016/j.dib.2018.06.113.
- [8] R. Ricci, R. Romagnoli, S. Montelpare, and D. Vitali, "Experimental study on a Savonius wind rotor for street lighting systems," *Applied Energy*, vol. 161. Elsevier Ltd, pp. 143–152, Jan. 01, 2016, doi: 10.1016/j.apenergy.2015.10.012.
- [9] M. A. Kamoji, S. B. Kedare, and S. V Prabhu, "Experimental Investigations on the Effect of Overlap Ratio and Blade Edge Conditions on the Performance of Conventional Savonius Rotor," *Wind Eng.*, vol. 32, no. 2, pp. 163–178, 2008, doi: 10.1260/030952408784815826.
- [10] Z. Driss, A. Damak, and M. S. Abid, "Evaluation of the Savonius Wind Rotor Performance for Different External Overlap Ratios," *Int. J. Fluid Mech. & Therm. Sci.*, vol. 1, no. 1, pp. 14–19, 2015.
- [11] M. Zemamou, M. Aggour, and A. Toumi, "Review of savonius wind turbine design and performance," in *Energy Procedia*, Dec. 2017, vol. 141, pp. 383–388, doi: 10.1016/j.egypro.2017.11.047.
- [12] W. A. El-Askary, A. S. Saad, A. M. AbdelSalam, and I. M. Sakr, "Investigating the performance of a twisted modified Savonius rotor," *J. Wind Eng. Ind. Aerodyn.*, vol. 182, pp. 344–355, Nov.

2018, doi: 10.1016/j.jweia.2018.10.009.

- [13] J. V. Akwa, G. Alves Da Silva Júnior, and A. P. Petry, "Discussion on the verification of the overlap ratio influence on performance coefficients of a Savonius wind rotor using computational fluid dynamics," *Renew. Energy*, vol. 38, no. 1, pp. 141–149, Feb. 2012, doi: 10.1016/j.renene.2011.07.013.
- [14] M. H. Mohamed, G. Janiga, E. Pap, and D. Thèvenin, "Optimization of Savonius turbines using an obstacle shielding the returning blade," *Renew. Energy*, vol. 35, no. 11, pp. 2618–2626, Nov. 2010, doi: 10.1016/j.renene.2010.04.007.
- [15] R. D. Maldonado *et al.*, "Design, simulation and construction of a Savonius wind rotor for subsidized houses in Mexico," in *Energy Procedia*, Jan. 2014, vol. 57, pp. 691–697, doi: 10.1016/j.egypro.2014.10.224.
- [16] B. D. Altan, M. Atilgan, and A. Özdamar, "An experimental study on improvement of a Savonius rotor performance with curtaining," *Exp. Therm. Fluid Sci.*, vol. 32, no. 8, pp. 1673–1678, Sep. 2008, doi: 10.1016/j.expthermflusci.2008.06.006.
- [17] E. Oguejiofor *et al.*, "Wind Deflection for Improvement of the Vertical Axis Wind Turbine," 2018.
- [18] S. Hadi *et al.*, "Study on performance improvement of the Savonius wind turbine for Urban Power System with Omni-Directional Guide Vane (ODGV)," *J. Adv. Res. Fluid Mech. Therm. Sci.*, vol. 55, no. 1, pp. 126–135, 2019.
- [19] K. M. Youssef, A. M. El Kholly, A. M. Hamed, N. A. Mahmoud, A. M. El Baz, and T. A. Mohamed, "An innovative augmentation technique of savonius wind turbine performance," *Wind Eng.*, vol. 44, no. 1, pp. 93–112, 2020.
- [20] M. Tartuferi, V. D'Alessandro, S. Montelpare, and R. Ricci, "Enhancement of Savonius wind rotor aerodynamic performance: a computational study of new blade shapes and curtain systems," *Energy*, vol. 79, pp. 371–384, 2015.
- [21] N. Alom and U. K. Saha, "Four decades of research into the augmentation techniques of Savonius wind turbine rotor," *J. Energy Resour. Technol.*, vol. 140, no. 5, 2018.
- [22] Fulan K. & Ayala C. Calentamiento global mas que un tema de moda. 2007.
- [23] Caballero, M., Lozano, S., & Ortega, B. (2007). Efecto invernadero, calentamiento global y cambio climático: una perspectiva desde las ciencias de la tierra. *Revista digital universitaria*, 8(10), 1-11.
- [24] Cipriano, J. (2011). *Alerta global*. Benchmark Education Company.
- [25] L. Merino, "Las energías renovables," *Energías Renovables para todos.*, vol. 1, no. 1, p. 20, 2012.
- [26] J. Moragues and A. Rapallini, "Energía eólica," *Inst. Argentino la Energía "General Mosconi*, vol. 22, 2003.
- [27] M. Elkhoury, T. Kiwata, and E. Aoun, "Experimental and numerical investigation of a three-dimensional vertical-axis wind turbine with variable-pitch," *J. Wind Eng. Ind. Aerodyn.*, vol. 139, pp. 111–123, Apr. 2015, doi: 10.1016/j.jweia.2015.01.004.

- [28] Y. T. Lin, P. H. Chiu, and C. C. Huang, "An experimental and numerical investigation on the power performance of 150 kW horizontal axis wind turbine," *Renew. Energy*, vol. 113, pp. 85–93, Dec. 2017, doi: 10.1016/j.renene.2017.05.065.
- [29] L. Chen, J. Chen, and Z. Zhang, "Review of the Savonius rotor's blade profile and its performance," *J. Renew. Sustain. Energy*, vol. 10, no. 1, p. 13306, 2018.
- [30] R. Kumar, K. Raahemifar, and A. S. Fung, "A critical review of vertical axis wind turbines for urban applications," *Renewable and Sustainable Energy Reviews*, vol. 89. Elsevier Ltd, pp. 281–291, Jun. 01, 2018, doi: 10.1016/j.rser.2018.03.033.
- [31] J. Chen, H. Yang, M. Yang, H. Xu, and Z. Hu, "A comprehensive review of the theoretical approaches for the airfoil design of lift-type vertical axis wind turbine," *Renewable and Sustainable Energy Reviews*, vol. 51. Elsevier Ltd, pp. 1709–1720, Aug. 11, 2015, doi: 10.1016/j.rser.2015.07.065.
- [32] Q. Li, T. Maeda, Y. Kamada, J. Murata, K. Furukawa, and M. Yamamoto, "Effect of number of blades on aerodynamic forces on a straight-bladed Vertical Axis Wind Turbine," *Energy*, vol. 90, pp. 784–795, Oct. 2015, doi: 10.1016/j.energy.2015.07.115.
- [33] A. P. Schaffarczyk, "Types of Wind Turbines," *Green Energy Technol.*, pp. 7–25, 2020, doi: 10.1007/978-3-030-41028-5_2.
- [34] S. J. Savonius, "The S-rotor and its applications," *Mech. Eng.*, vol. 53, no. 5, pp. 333–338, 1931.
- [35] S. Roy and U. K. Saha, "Review of experimental investigations into the design, performance and optimization of the Savonius rotor," *Proc. Inst. Mech. Eng. Part A J. Power Energy*, vol. 227, no. 4, pp. 528–542, 2013.
- [36] L. C. Valdès and K. Raniriharinosy, "Low technical wind pumping of high efficiency," *Renew. Energy*, vol. 24, no. 2, pp. 275–301, Oct. 2001, doi: 10.1016/S0960-1481(00)00201-9.
- [37] J. L. Menet, L. C. Valdès, and B. Ménart, "A comparative calculation of the wind turbines capacities on the basis of the L- σ criterion," *Renew. Energy*, vol. 22, no. 4, pp. 491–506, Apr. 2001, doi: 10.1016/S0960-1481(00)00114-2.
- [38] W. Tian, Z. Mao, B. Zhang, and Y. Li, "Shape optimization of a Savonius wind rotor with different convex and concave sides," *Renew. Energy*, vol. 117, pp. 287–299, Mar. 2018, doi: 10.1016/j.renene.2017.10.067.
- [39] F. Wenehenubun, A. Saputra, and H. Sutanto, "An experimental study on the performance of Savonius wind turbines related with the number of blades," *Energy Procedia*, vol. 68, pp. 297–304, 2015, doi: 10.1016/j.egypro.2015.03.259.
- [40] N. Alom, B. Borah, and U. K. Saha, "An insight into the drag and lift characteristics of modified Bach and Benesh profiles of Savonius rotor," in *Energy Procedia*, Jul. 2018, vol. 144, pp. 50–56, doi: 10.1016/j.egypro.2018.06.007.
- [41] C. M. Chan, H. L. Bai, and D. Q. He, "Blade shape optimization of the Savonius wind turbine using a genetic algorithm," *Appl. Energy*, vol. 213, pp. 148–157, Mar. 2018, doi: 10.1016/j.apenergy.2018.01.029.
- [42] M. Mari, M. Venturini, and A. Beyene, "A novel geometry for vertical axis wind turbines based

on the Savonius concept,” *J. Energy Resour. Technol.*, vol. 139, no. 6, 2017.

- [43] N. Alom, S. C. Kolaparthi, S. C. Gadde, and U. K. Saha, “Aerodynamic design optimization of elliptical-bladed Savonius-Style wind turbine by numerical simulations,” in *International Conference on Offshore Mechanics and Arctic Engineering*, 2016, vol. 49972, p. V006T09A009.
- [44] N. Alom and U. K. Saha, “Influence of blade profiles on Savonius rotor performance: Numerical simulation and experimental validation,” *Energy Convers. Manag.*, vol. 186, pp. 267–277, Apr. 2019, doi: 10.1016/j.enconman.2019.02.058.
- [45] I. Marinić-Kragić, D. Vučina, and Z. Milas, “Concept of flexible vertical-axis wind turbine with numerical simulation and shape optimization,” *Energy*, vol. 167, pp. 841–852, Jan. 2019, doi: 10.1016/j.energy.2018.11.026.
- [46] “A proposed, three-sail, savonius-type wind-rotor.” .
- [47] P. D. Fleming, S. D. Probert, and D. Tanton, “Designs and performances of flexible and taut sail Savonius-type wind-turbines,” *Appl. Energy*, vol. 19, no. 2, pp. 97–110, 1985.
- [48] P. Ghosh, M. A. Kamoji, A. W. Date, and S. V Prabhu, “Experimental Investigations on Sail Type Wind-Turbines,” *Wind Eng.*, vol. 33, no. 4, pp. 349–359, 2009.
- [49] H. Ersoy and S. Yalcindag, “An experimental study on the improvement of Savonius turbine performance using flexible sails,” *Int. J. green energy*, vol. 11, no. 8, pp. 796–807, 2014.
- [50] K. Sobczak, D. Obidowski, P. Reorowicz, and E. Marchewka, “Numerical investigations of the savonius turbine with deformable blades,” *Energies*, vol. 13, no. 14, p. 3717, 2020.
- [51] M. O. L. Hansen, *Aerodynamics of wind turbines*. Routledge, 2015.
- [52] M. B. Patel and V. Kevat, “Performance prediction of straight bladed Darrieus wind turbine by single streamtube model,” *Int. J. Adv. Eng. Technol.*, vol. 14, p. 2, 2013.
- [53] I. Paraschivoiu, “Double-multiple streamtube model for studying vertical-axis wind turbines,” *J. Propuls. power*, vol. 4, no. 4, pp. 370–377, 1988.
- [54] H. Jang, I. Paek, S. Kim, and D. Jeong, “Performance Prediction and Validation of a Small-Capacity Twisted Savonius Wind Turbine,” *Energies*, vol. 12, no. 9, p. 1721, 2019.
- [55] I. Dobrev and F. Massouh, “CFD and PIV investigation of unsteady flow through Savonius wind turbine,” in *Energy Procedia*, Jan. 2011, vol. 6, pp. 711–720, doi: 10.1016/j.egypro.2011.05.081.
- [56] N. Thakur, A. Biswas, Y. Kumar, and M. Basumatary, “CFD analysis of performance improvement of the Savonius water turbine by using an impinging jet duct design,” *Chinese J. Chem. Eng.*, vol. 27, no. 4, pp. 794–801, Apr. 2019, doi: 10.1016/j.cjche.2018.11.014.
- [57] P. Jaohindy, S. McTavish, F. Garde, and A. Bastide, “An analysis of the transient forces acting on Savonius rotors with different aspect ratios,” *Renew. Energy*, vol. 55, pp. 286–295, Jul. 2013, doi: 10.1016/j.renene.2012.12.045.
- [58] S. Mauro, S. Brusca, R. Lanzafame, and M. Messina, “CFD modeling of a ducted Savonius wind turbine for the evaluation of the blockage effects on rotor performance,” *Renew. Energy*, vol. 141, pp. 28–39, Oct. 2019, doi: 10.1016/j.renene.2019.03.125.

- [59] S. C. Goh, S. R. Boopathy, C. Krishnaswami, and J. U. Schlüter, "Tow testing of Savonius wind turbine above a bluff body complemented by CFD simulation," *Renew. Energy*, vol. 87, pp. 332–345, Mar. 2016, doi: 10.1016/j.renene.2015.10.015.
- [60] G. Ferrari, D. Federici, P. Schito, F. Inzoli, and R. Mereu, "CFD study of Savonius wind turbine: 3D model validation and parametric analysis," *Renew. Energy*, vol. 105, pp. 722–734, May 2017, doi: 10.1016/j.renene.2016.12.077.
- [61] P. Larin, M. Paraschivoiu, and C. Aygun, "CFD based synergistic analysis of wind turbines for roof mounted integration," *J. Wind Eng. Ind. Aerodyn.*, vol. 156, pp. 1–13, Sep. 2016, doi: 10.1016/j.jweia.2016.06.007.
- [62] F. R. Menter, M. Kuntz, and R. Langtry, "Ten years of industrial experience with the SST turbulence model," *Turbul. heat mass Transf.*, vol. 4, no. 1, pp. 625–632, 2003.
- [63] A. Hellsten, "Some improvements in Menter's k-omega SST turbulence model," in *29th AIAA, Fluid Dynamics Conference*, 1998, p. 2554.
- [64] L.-S. Paraschiv, S. Paraschiv, and I. V Ion, "Investigation of wind power density distribution using Rayleigh probability density function," *Energy Procedia*, vol. 157, pp. 1546–1552, 2019.
- [65] J. F. Manwell, J. G. McGowan, and A. L. Rogers, *Wind energy explained: theory, design and application*. John Wiley & Sons, 2010.
- [66] I. Troen and E. Lundtang Petersen, "European wind atlas," 1989.
- [67] T. P. Chang, "Estimation of wind energy potential using different probability density functions," *Appl. Energy*, vol. 88, no. 5, pp. 1848–1856, 2011.
- [68] L. Corona, G. Abarca, and J. Mares, "Sensores y actuadores: aplicaciones con Arduino," *Mex. Grup. Editor. Patria*, 2014.
- [69] F. Valdés and R. P. Areny, *Microcontroladores fundamentos y aplicaciones con PIC*, vol. 1149. Marcombo, 2007.
- [70] M. McRoberts, *Beginning Arduino*. Apress, 2011.
- [71] Di Eben Upton, Gareth Halfacree, "Raspberry Pi User Guide" Third Edition, Chapter 1, 2014
- [72] F. Torres and C. A. Jara, "Sensores y detectores," *Automatización*, 2011.
- [73] A. J. Alexander and B. P. Holownia, "Wind tunnel tests on a savonius rotor," *J. Wind Eng. Ind. Aerodyn.*, vol. 3, no. 4, pp. 343–351, Jan. 1978, doi: 10.1016/0167-6105(78)90037-5.
- [74] N. H. Mahmoud, A. A. El-Haroun, E. Wahba, and M. H. Nasef, "An experimental study on improvement of Savonius rotor performance," *Alexandria Eng. J.*, vol. 51, no. 1, pp. 19–25, Mar. 2012, doi: 10.1016/j.aej.2012.07.003.
- [75] M. H. Ali and others, "Experimental comparison study for Savonius wind turbine of two & three blades at low wind speed," *Int. J. Mod. Eng. Res.*, vol. 3, no. 5, pp. 2978–2986, 2013.
- [76] S. Roy and U. K. Saha, "An adapted blockage factor correlation approach in wind tunnel experiments of a Savonius-style wind turbine," *Energy Convers. Manag.*, vol. 86, pp. 418–427, 2014.
- [77] J. A. Castillo, "Atlas Interactivo - Vientos," *IDEAM*. 2015, [Online]. Available:

<http://atlas.ideam.gov.co/visorAtlasVientos.html>.